

(Amino)cyclophosphazenes as Multisite Ligands for the Synthesis of Antitumoral and Antibacterial Silver(I) Complexes

Elena Gascón, Sara Maisanaba, Isabel Ota, Eva Valero, Guillermo Repetto, Peter G. Jones, and Josefina Jiménez*

Cite This: <https://dx.doi.org/10.1021/acs.inorgchem.9b03334>

Read Online

ACCESS |



Metrics & More

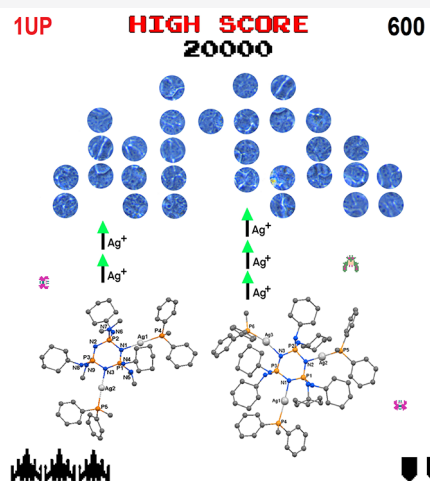


Article Recommendations



Supporting Information

ABSTRACT: The reactivity of the multisite (amino)cyclotriphosphazene ligands, $[\text{N}_3\text{P}_3(\text{NHCy})_6]$ and $[\text{N}_3\text{P}_3(\text{NHCy})_3(\text{NMe}_2)_3]$, has been explored in order to obtain silver(I) metallophosphazene complexes. Two series of cationic silver(I) metallophosphazenes were obtained and characterized: $[\text{N}_3\text{P}_3(\text{NHCy})_6\{\text{AgL}\}_n](\text{TfO})_n$ [$n = 2$, $\text{L} = \text{PPh}_3$ (2), PPh_2Me (4); $n = 3$, $\text{L} = \text{PPh}_3$ (3), PPh_2Me (5), TPA ($\text{TPA} = 1,3,5\text{-triazia-7-phosphaadamantane}$, 6)] and *nongem-trans*- $[\text{N}_3\text{P}_3(\text{NHCy})_3(\text{NMe}_2)_3\{\text{AgL}\}_n](\text{TfO})_n$ [$n = 2$, $\text{L} = \text{PPh}_3$ (7), PPh_2Me (9); $n = 3$, $\text{L} = \text{PPh}_3$ (8), PPh_2Me (10)]. 5, 7, and 9 have also been characterized by single-crystal X-ray diffraction, thereby allowing key bonding information to be obtained. Compounds 2–6, 9, and 10 were screened for in vitro cytotoxic activity against two tumor human cell lines, MCF7 (breast adenocarcinoma) and HepG2 (hepatocellular carcinoma), and for antimicrobial activity against five bacterial species including Gram-positive, Gram-negative, and Mycobacteria strains. Both the IC_{50} and MIC values revealed excellent biological activity for these metal complexes, compared with their precursors and cisplatin and also AgNO_3 and silver sulfadiazine, respectively. Both IC_{50} and MIC values are among the lowest values found for any silver derivatives against the cell lines and bacterial strains used in this work. The structure–activity relationships were clear. The most cytotoxic and antimicrobial derivatives were those with the triphenylphosphane and $[\text{N}_3\text{P}_3(\text{NHCy})_6]$ ligands. A significant improvement in the activity was also observed upon a rise in the number of silver atoms linked to the phosphazene ring.



1. INTRODUCTION

Over the years, there has been continuous interest in the biological activity of metal complexes. Among them, silver has been used for numerous medical conditions, mostly because of its antibacterial activity.¹ The antibacterial, antifungal, and antiviral properties of silver ions, silver compounds, and, recently, silver nanoparticles have been extensively studied, and these topics have been thoroughly reviewed.^{2,3} Nowadays the preparation of novel antibacterial agents has become a priority because of the presence of multidrug-resistant pathogens.⁴ *Mycobacterium tuberculosis* (the organism causing tuberculosis that still wreaks havoc in both developed and undeveloped countries) aside, *Staphylococcus aureus* (resistant to methicillin, MRSA), *Escherichia coli*, and *Pseudomonas aeruginosa*, among others, are becoming more and more resistant, and the lack of efficient treatment is one of the leading causes of high mortality rates.⁵ Although the antimicrobial activity mechanism of silver(I) complexes has not been well established,^{2a,6} microorganisms are unlikely to develop resistance against silver compared to antibiotics because silver attacks a broad range of targets in the microbes, and only a few accounts of resistance have been reported.⁷ What is more, silver is also found to be

nontoxic to humans in minute concentrations.⁸ The most widely used silver reagents have been in the form of inorganic salts or complexes, such as silver nitrate and silver sulfadiazine, and in combination with proteins. Actually, silver sulfadiazine works as a broad-spectrum antibiotic used mainly in the treatment of burn wounds. However, almost all of the current clinical silver agents have their own disadvantages, limiting their clinical usefulness. Therefore, on the basis of the benefits of silver, the pressing interest in finding new silver pharmaceuticals promoted the development of more efficient and convenient silver agents, in which employing ligands that can strongly coordinate to the active silver(I) ions is essential.^{2f} In recent years, the systematic discovery and development of silver complexes has yielded a large number of promising antibacterial, antifungal, and even anticancer compounds, and several reviews on the topics have been reported. Recently,

Received: November 13, 2019



Lobana et al. performed an in vitro antimicrobial potential and biosafety evaluation of silver(I) derivatives of several thio ligands, some of which have shown significant antimicrobial activity and low cellular toxicity with a high percent of cell viability.^{9a–c} Banti and Hadjikakou reviewed the antiproliferative activity of silver(I) compounds^{9d} in comparison with that of cisplatin, a clinical chemotherapeutic drug currently in use. Liang et al. also recently reviewed the advances in the medical use of silver complexes.^{2f} Other more general reviews concerning metallodrugs have also recently been reported.^{5,10} These surveys show that silver(I) complexes exhibit selectivity against a variety of cancer cells and bacterial strains with regard to the kinds of ligands coordinated to silver(I) ions. However, the research in this field is still limited at present. Most studies focus on silver(I) N-heterocyclic carbene complexes.¹¹ New ligands for better activity and lower toxicity need to be studied further. Besides, more research is still required to fully elucidate the mechanism of action of silver(I) complexes against both microorganism and tumor cells.⁵

Since its synthesis for the first time in 1834, hexachlorocyclotriphosphazene, $[\text{N}_3\text{P}_3\text{Cl}_6]$, has been an important compound of phosphorus chemistry as a scaffold, and a large number of cyclotriphosphazene (CPZ) derivatives and their analogue polymers, polyphosphazenes (PPZs), have been synthesized and applied in various fields such as biology, catalysis, fluorescence, nanomaterials, etc.¹² Today, one of the most important uses concerns its biomedical applications.¹³ Phosphazenes comprise a broad class of molecules based on the repeating unit $[\text{NPR}_2]$ and include cyclic or linear oligomers and polymers. The most striking characteristic of this type of compound is its associated synthetic versatility, which enables the introduction of almost any substituent group R at phosphorus and allows its properties to be tailored by the choice of appropriate functional groups.¹² Notably, biocompatibility and biodegradability can be regulated by the introduction of specific side groups, R.¹⁴ The degradation rate can also be controlled by external stimuli, such as the temperature, radiation, pH of the degradation medium, and degradation product solubility.¹⁴ Nowadays, the use of PPZs in drug-delivery applications, especially proteins and anticancer drug delivery, has become a significant focus.^{13b,15} The effects of various side groups on the properties of the resultant PPZs and their use in different approaches, such as drug delivery, have recently been reviewed.^{13b} Macromolecular prodrugs are known to show excellent tumor-targeting properties by their enhanced permeability and retention effect¹⁶ and exhibit improved body distribution and prolonged blood circulation because of the dominant pharmacokinetic properties of the macromolecular carrier.¹⁷ In this respect, drugs can be physically encapsulated by liposomes, nanocapsules, or polymeric micelles or vesicles and, alternatively, conjugated to linear polymers or dendrimers by covalent bonding. Drug–polymer conjugates are an emerging area of drug delivery in order to combat the hurdles related to the delivery of drugs such as low solubility, protection against degradation by various factors, low bioavailability, and high dose toxicity. Thus, some antibiotic, antiviral, antitumoral, or antimalarial drugs have been conjugated to PPZs and CPZs.¹³ CPZs are even in a much better position than PPZs because the phosphazene trimer backbone is monodisperse and it is much easier to control the purity and molecular weight of these molecules,^{13a} which both play a critical role for its clinical use. Besides, CPZs can be used as the core of dendrimers, giving

rise to a wide variety of branched molecules that have precise structure and are also monodisperse.¹⁸ Over the past few years, CPZs have been developed in several pharmacological domains,¹⁹ and the use of dendrimers, in general, and dendrimers based on the CPZ core, in particular, has been said to represent a new strategy in nanomedicine. Recent developments of CPZs for major pharmaceutical applications have been reviewed by Majoral et al.^{13c} Besides, both PPZs and CPZs can be used as scaffolds for the design and construction of a variety of ligands,^{12c,20} to coordinate to metallic drugs. The facile substitution of P–Cl bonds in the cyclic trimer hexachlorocyclotriphosphazene, $[\text{N}_3\text{P}_3\text{Cl}_6]$, allows the ready construction of cyclophosphazenes carrying additional exocyclic donor functions, giving a library of multisite coordination ligands. Furthermore, the ring nitrogen atoms have sufficient basicity to coordinate to metals depending on the electronic properties of the exocyclic substituents at phosphorus. Alkyl, aryl, and primary and secondary organoamino substituents enhance the donor ability of ring nitrogen atoms.^{20c}

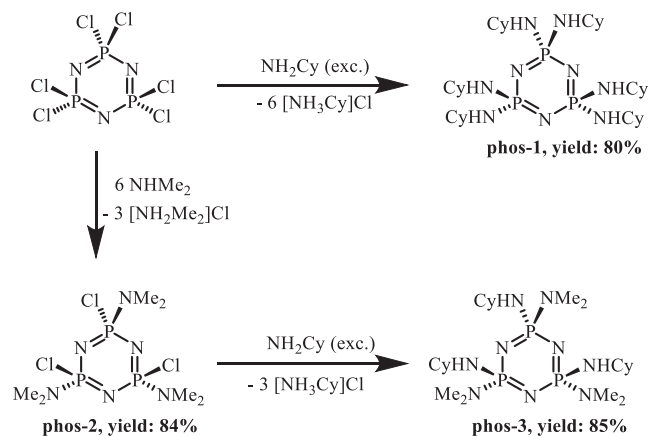
Several authors have prepared and studied the tumoral properties of cyclophosphazene- or polyphosphazeneplatinum-(II) conjugates.²¹ Recently, Henke et al. introduced PPZ-based anticancer prodrug conjugates in which cisplatin and oxaliplatin were first converted into prodrugs and then attached to the PPZ through a linker.²² Silver derivatives of phosphazenes (cyclic or polymers) are also known.²³ The Steiner group has published interesting work using (amino)-cyclophosphazenes to prepare structurally characterized silver-(I) coordination polymers by the formation of linear N–Ag–N connections via nitrogen centers of the phosphazene ring.²⁴ We have also contributed to this field by reporting CPZs and PPZs containing gold or silver and their thermolytic transformation into nanostructured materials or into metallic micro- and nanostructures deposited on silicon and silica surfaces.²⁵ PPZs and CPZs decorated with silver nanoparticles have also been synthesized.²⁶ However, to the best of our knowledge, there are no reports of silver phosphazenes with biological properties, such as the antimicrobial or antitumoral ones. Thus, the interesting biological properties of both silver(I) complexes and phosphazenes, discussed above, together with our experience in the chemistry of both silver and phosphazenes, prompted us to prepare new silver cyclotriphosphazenes and study their antimicrobial and antitumoral properties.

Herein, the reactivity of the multiside (amino)-cyclotriphosphazene ligands, $[\text{N}_3\text{P}_3(\text{NHCy})_6]$ and $[\text{N}_3\text{P}_3(\text{NHCy})_3(\text{NMe}_2)_3]$, has been explored in order to obtain silver(I) metallophosphazene complexes. For this purpose, the simple strategy used was to employ silver(I) precursors bearing a phosphane ligand and a labile triflate (OTf) to be displaced by the phosphazene ligand. Thus, two series of silver(I) metallophosphazenes were obtained, and studies of their anticancer activity in the human breast adenocarcinoma (MCF7) and human hepatocellular carcinoma (HepG2) cell lines were carried out. The antibacterial activity was also tested against the Gram-negative strains *E. coli* and *P. aeruginosa*, against the Gram-positive strain *S. aureus*, and against two *M. tuberculosis* complex (MTBC) strains, *M. tuberculosis* H37Rv and *M. bovis* BCG Pasteur. Comparisons with the corresponding antiproliferative and antimicrobial activity of cisplatin and silver(I) nitrate, respectively, were also performed.

2. RESULTS AND DISCUSSION

2.1. Synthesis and Characterization of the Starting CPZs. Syntheses of the starting CPZs are outlined in Scheme 1.

Scheme 1. Syntheses of the Starting CPZs

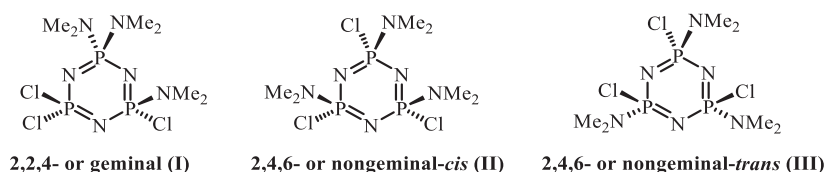


Specifically, the starting CPZs, a single-substituent trimer, $[\text{N}_3\text{P}_3(\text{NHCy})_6]$ (**phos-1**), and a mixed-substituent trimer, *nongem-trans*- $[\text{N}_3\text{P}_3(\text{NHCy})_3(\text{NMe}_2)_3]$ (**phos-3**), were both prepared in high yield (>80%) from $[\text{N}_3\text{P}_3\text{Cl}_6]$ and *nongem-trans*- $[\text{N}_3\text{P}_3\text{Cl}_3(\text{NMe}_2)_3]$ (**phos-2**), respectively, using tetrahydrofuran as a solvent and cyclohexylamine as a nucleophile and a base (see the [Experimental Section](#)). The syntheses of **phos-1** and **phos-2** were described previously,^{27–29} starting from hexachlorocyclotriphosphazene, $[\text{N}_3\text{P}_3\text{Cl}_6]$, but involving less efficient methods than those used by us. The trimer **phos-1** was prepared by Chandrasekhar et al. using diazabicycloundecane as a base and chloroform as a solvent.^{27,28} In this reaction, the major product was the incompletely substituted derivative $[\text{N}_3\text{P}_3\text{Cl}_2(\text{NHCy})_4]$ and only prolonged reaction conditions (8 days of heating under reflux) led to the fully single-substituted derivative **phos-1**, which was formed in only minor yield (6.8%).²⁷ Compound **phos-2** was synthesized by Ford et al. using diethyl ether as a solvent at room temperature (RT; yield 27%) and by Keat and Shaw at -78°C (yield 49%).²⁹ Starting also from $[\text{N}_3\text{P}_3\text{Cl}_6]$ but using tetrahydrofuran as a solvent and with the slow dropwise addition of dimethylamine as a nucleophile and a base at 0°C , we obtained **phos-2** in high yield (84%; see the [Experimental Section](#) for details). The substitution reaction of $[\text{N}_3\text{P}_3\text{Cl}_6]$ has been extensively studied, with primary interest in the regio- and stereochemical pathways.^{30,31} In particular, partial substitution of hexachlorocyclotriphosphazene usually results not only in stoichiometrically different products but also in various geometrical and positional isomers that are not easy to separate. Thus, reactions leading to the trisubstituted material $[\text{N}_3\text{P}_3\text{Cl}_3\text{X}_3]$ usually result in the formation of not only trisubstituted regioisomers,

i.e., 2,2,4- and 2,4,6- (numbering starts at the nitrogen atom), which are also referred to as geminal and nongeminal isomers, respectively, but also di- and tetrasubstituted derivatives as minor products. Besides, the nongeminal materials can exist in two stereoisomeric forms, either with the three substituents on the same side of the mean plane of the phosphazene ring (nongeminal *cis*-2,4,6) or with two on one side and the third on the other (nongeminal *trans*-2,4,6) (see [Chart 1](#)).

As reported, some of the variations in the aminolysis patterns may be associated with the experimental conditions, such as the temperature, solvent, and stoichiometry, which in some circumstances may determine the presence or absence of a particular isomer or at least its relative proportions.³⁰ All three compounds that we obtained, **phos-1** to **phos-3**, were completely characterized by elemental analysis, IR, ^1H , $^{13}\text{C}\{^1\text{H}\}$, and $^{31}\text{P}\{^1\text{H}\}$ NMR spectroscopy, and mass spectrometry (MS).³² All of these data are given in the [Experimental Section](#) and are consistent with the formulas and structures indicated. Specifically, **phos-2** has a nongeminal *trans* trisubstituted configuration. That nongeminal *trans* configuration is maintained in the new phosphazene **phos-3** after complete substitution of the chlorine atoms by the cyclohexylamino units. Elemental analysis and MS indicated that the compositions of **phos-2** and **phos-3** are $[\text{N}_3\text{P}_3\text{Cl}_3(\text{NMe}_2)_3]$ and $[\text{N}_3\text{P}_3(\text{NHCy})_3(\text{NMe}_2)_3]$, respectively, and ^1H and $^{31}\text{P}\{^1\text{H}\}$ NMR spectroscopy indicated that both have a nongeminal *trans* configuration. NMR spectroscopy is one of the most powerful tools for the structural characterization of cyclophosphazenes because the most critical structural information is available from the chemical shifts and spin–spin coupling data of their $^{31}\text{P}\{^1\text{H}\}$ NMR spectra.^{30,33,34} Thus, the $^{31}\text{P}\{^1\text{H}\}$ NMR spectra of **phos-2** and **phos-3** showed a multiplet from a spin system AB_2 , which indicates that both of them are nongeminal *trans* (see [Figure 1a](#) for **phos-2** and [Figure 2a](#) for **phos-3**). The geminal trisubstituted derivative (I in [Chart 1](#)) would have exhibited a spin system AX_2 , i.e., a doublet and a triplet (both phosphorus atoms would have markedly different environments), and the nongeminal *cis* trisubstituted derivative (II in [Chart 1](#)) a spin system A_3 , i.e., a singlet. The ^1H NMR spectra of all of the dimethylaminolysis products of $[\text{N}_3\text{P}_3\text{Cl}_6]$ have been examined elsewhere,²⁹ as have those of the trisubstituted derivatives including **phos-2**. As the authors commented,²⁹ detailed interpretation of the ^1H NMR spectra is difficult because of their great complexity. At their simplest, when they contain only one type of dimethylamino environment, the spectrum consists of one doublet centered at approximately 2.50–2.70 ppm (with an additional broadened structure between the major peaks),³⁵ with a separation (apparent coupling constant, $J'(\text{P}-\text{H})$ or N) varying between 11 and 18 Hz. The N value is dependent on the nature of the second substituent bonded directly to the phosphorus carrying the $-\text{NMe}_2$ group. A $\text{P}(\text{Cl})(\text{NMe}_2)$ group gives an N value of about 18 Hz, and a $\text{P}(\text{NMe}_2)_2$ or $\text{P}(\text{NR}_2)(\text{NMe}_2)$ group gives about 11 Hz.²⁹ Thus, the coupling

Chart 1. Trisubstituted CPZ Isomers



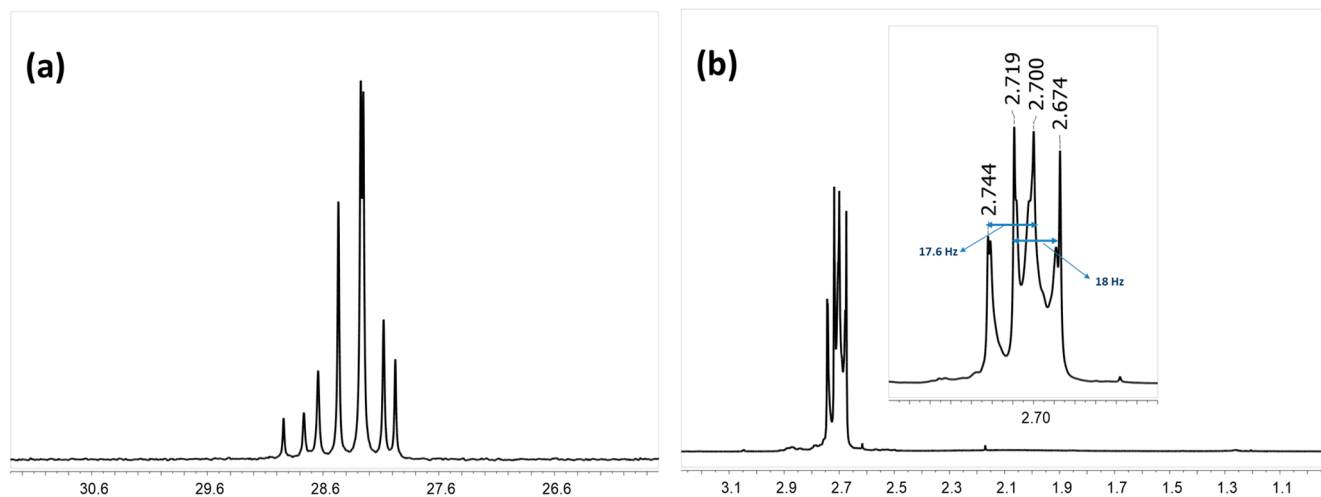


Figure 1. (a) $^{31}\text{P}\{^1\text{H}\}$ and (b) ^1H NMR spectra of compound **phos-2** in CDCl_3 .

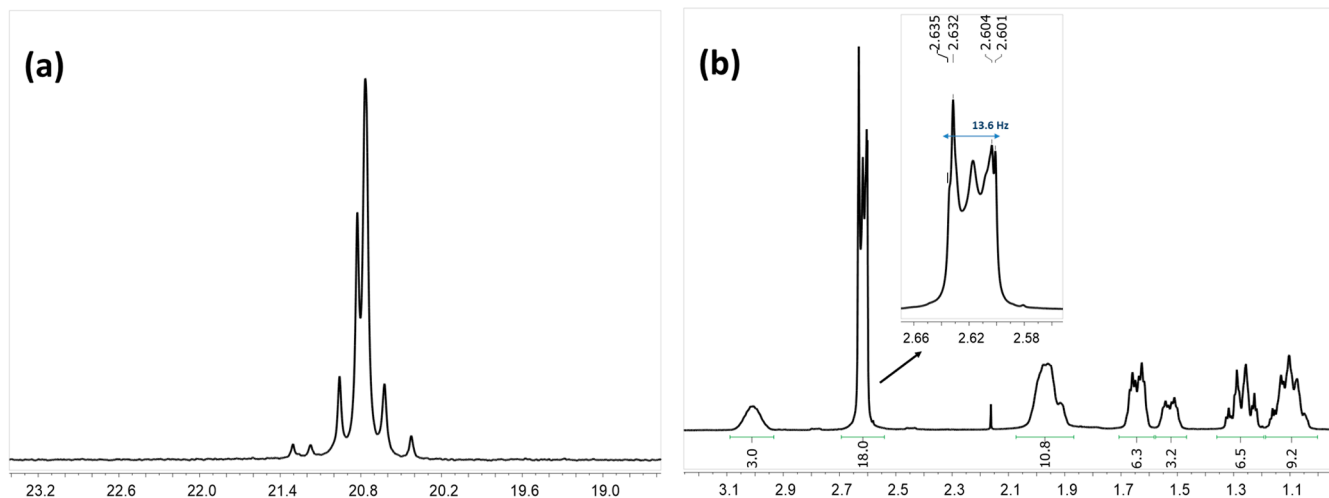
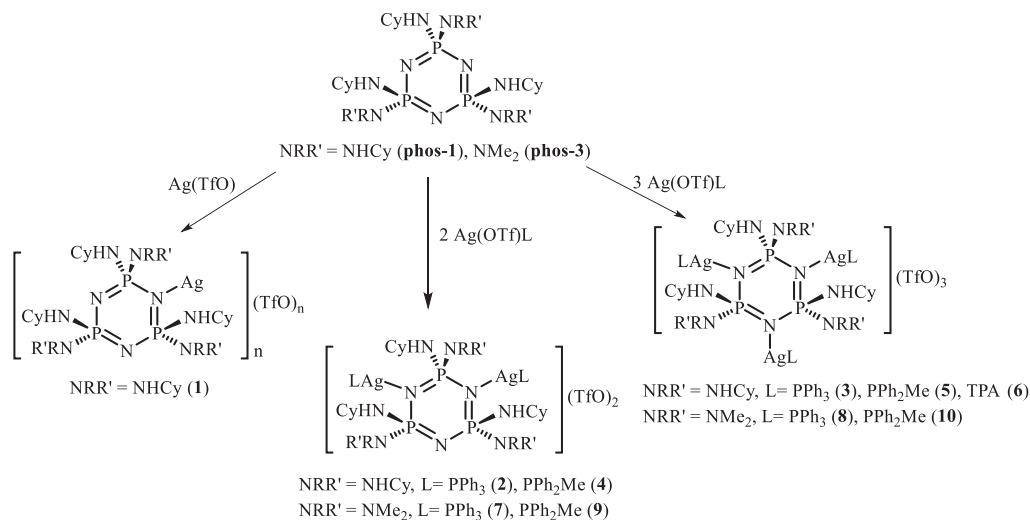


Figure 2. (a) $^{31}\text{P}\{^1\text{H}\}$ and (b) ^1H NMR spectra of compound **phos-3** in CDCl_3 .

Scheme 2. Synthesis of New Metallophosphazenes



constants indicate the groups attached to the phosphorus atoms, and the number of doublets indicates different sets of

environments. The ^1H NMR spectrum of **phos-2** showed two pseudodoublets, each with N of approximately 18 Hz (see

Figure 1b), as reported in the literature.^{29a} This N value is in accordance with the fact that the $-\text{NMe}_2$ groups are each located on a separate phosphorus atom (nongeminal derivative), i.e., $\text{P}(\text{Cl})(\text{NMe}_2)$ groups. The presence of two pseudodoublets confirms that **phos-2** is the trans isomer. The ^1H NMR spectrum of the new phosphazene **phos-3** is shown in Figure 2b, which presents the signals corresponding to the cyclohexylamino and dimethylamino units. For dimethylamino protons, a multiplet centered at 2.62 ppm is observed with $N = 13.6$ Hz. As mentioned before, this N value is in accordance with the presence of $\text{P}(\text{NR}_2)(\text{NMe}_2)$ groups.

2.2. Synthesis and Characterization of the Metallophosphazenes. The reaction of **phos-1** or **phos-3** with the silver complexes $[\text{Ag}(\text{OTf})\text{L}]$ ($\text{OTf} = \text{OSO}_2\text{CF}_3$; $\text{L} = \text{PPh}_3$, PPh_2Me , or TPA , where $\text{TPA} = 1,3,5\text{-triaz-7-phosphaadamantane}$) in dichloromethane and in different molar ratios of 1:2 or 1:3 led to two series of cationic metallophosphazenes, $[\text{N}_3\text{P}_3(\text{NHCy})_6\{\text{AgL}\}_n](\text{TfO})_n$ [$n = 2$, $\text{L} = \text{PPh}_3$ (**2**), PPh_2Me (**4**); $n = 3$, $\text{L} = \text{PPh}_3$ (**3**), PPh_2Me (**5**), TPA (**6**)] and *nongem-trans*- $[\text{N}_3\text{P}_3(\text{NHCy})_3(\text{NMe}_2)_3\{\text{AgL}\}_n](\text{TfO})_n$ [$n = 2$, $\text{L} = \text{PPh}_3$ (**7**), PPh_2Me (**9**); $n = 3$, $\text{L} = \text{PPh}_3$ (**8**), PPh_2Me (**10**)]. In all of them, the silver groups “ AgL ” are coordinated to the nitrogen atoms of the phosphazene ring, whereby their number (2 or 3) depends on the molar ratio used (see Scheme 2). The reaction of **phos-1** with the same starting complexes, $[\text{Ag}(\text{OTf})\text{L}]$ ($\text{L} = \text{PPh}_3$ or PPh_2Me), but in a molar ratio of 1:1 evolved in a more complex way, giving a mixture of compounds in which the major product was $[\text{N}_3\text{P}_3(\text{NHCy})_6\text{Ag}(\text{TfO})]_n$ (**1**). The identification of this derivative **1** was confirmed by the reaction of **phos-1** with AgTfO in a molar ratio of 1:1 (see the Experimental Section).

All new metallophosphazenes **2–10** were obtained in high yield and could be handled and stored protected from light under ambient conditions for large periods of time. They are soluble in dichloromethane, acetone, chloroform, and dimethyl sulfoxide (DMSO) and only slightly soluble or insoluble in hexane or pentane. Their solutions must also be handled and stored protected from light, and they were stable for at least 1 week at RT under these conditions, as was proven by $^{31}\text{P}\{^1\text{H}\}$ and ^1H NMR spectroscopy. All of them are insoluble in water, even compound **6**, bearing the water-soluble phosphane ligand TPA , which was prepared in an unsuccessful attempt to obtain a water-soluble metallophosphazene. Compound **1** is only sparingly soluble in dichloromethane, chloroform, or acetone and insoluble in water, diethyl ether, ethanol, hexane, or pentane. All of the compounds **1–10** were characterized by elemental analysis, IR, ^1H , $^{13}\text{C}\{^1\text{H}\}$, and $^{31}\text{P}\{^1\text{H}\}$ NMR spectroscopy, and MS. All of these data are given in the Experimental Section and are consistent with the formulas and structures indicated and, specifically, with the coordination of metals to the backbone nitrogen atoms. In addition, X-ray structural analyses of **5**, **7**, and **9** confirmed the proposed structures.

IR spectra of all of these complexes clearly evidence coordination of the metal fragments, AgL , to **phos-1** or **phos-3**. Thus, the IR spectra show absorptions attributable to trifluoromethanesulfonate (triflate) units and to the phosphane ligands, which are all shifted from those in the starting complexes $[\text{Ag}(\text{OTf})\text{L}]$ ($\text{L} = \text{PPh}_3$, PPh_2Me , or TPA). The triflate peaks, which could, in principle, be used to distinguish covalent and ionic trifluoromethanesulfonate,³⁶ are not very useful because an unambiguous assignment is hindered by the overlap of CF_3 , SO_3 , and phosphane vibrational modes.³⁷

However, all of the **1–10** complexes have very similar bands in shape and position in the stretching region of the triflate ($1280\text{--}1000\text{ cm}^{-1}$, $\nu[\text{SO}_3(\text{E})]$, $\nu[\text{SO}_3(\text{A}_1)]$, $\nu[\text{CF}_3(\text{A}_1)]$, and $\nu[\text{CF}_3(\text{E})]$; see the Experimental Section). This is consistent with the presence of ionic trifluoromethanesulfonate, which was clearly confirmed in **7** and **9** by X-ray structural analyses. Besides, a single peak at approximately -78 ppm appears in the ^{19}F NMR spectra of all synthesized complexes. The bands of the characteristic phosphazene absorptions in the IR spectra, such as $\text{P}=\text{N}$ and $\text{C}-\text{N}$ (at 1186 and 1177 cm^{-1} in **phos-1** and 1180 , 1171 , and 1140 cm^{-1} in **phos-3**), change after coordination of the metal, as previously observed in other metallophosphazenes with silver coordinated to the backbone nitrogen atoms.^{23c} However, new bands corresponding to these peak frequencies could not be assigned because of overlap with CF_3 , SO_3 , and phosphane vibrational modes. The bands in the $3000\text{--}3400\text{ cm}^{-1}$ region, which are assigned to the $\text{N}-\text{H}$ stretching, are also different from those of the starting phosphazenes. Upon complexation, only one band at approximately 3300 cm^{-1} is observed for all complexes.

The $^{31}\text{P}\{^1\text{H}\}$ and ^1H NMR spectra in solution are also consistent with coordination of the metal fragments to the ring nitrogen atoms. The signals observed for **2–6**, with the single-substituent trimer **phos-1**, in their $^{31}\text{P}\{^1\text{H}\}$ NMR spectra at RT, are collected in Table 1. A single peak, shifted downfield

Table 1. $^{31}\text{P}\{^1\text{H}\}$ NMR Spectroscopic Data for **2–6** and Starting Products^a

compound	$\delta[\text{N}-\text{P}-\text{N}]$	$\frac{\delta[\text{PR}_3]}{[^1\text{J}(^{109}\text{Ag}-\text{P})]^{1/3} [^1\text{J}(^{107}\text{Ag}-\text{P})]^{2/3}}$ ^b
$[\text{N}_3\text{P}_3(\text{NHCy})_6]$ (phos-1)	14.44 (s)	
$[\text{Ag}(\text{OTf})\text{PPh}_3]$		16.79 (br)
$[\text{N}_3\text{P}_3(\text{NHCy})_6\{\text{AgPPh}_3\}_2](\text{TfO})_2$ (2)	16.90 (br)	17.12 (dd) [746.1], [653.4]
$[\text{N}_3\text{P}_3(\text{NHCy})_6\{\text{AgPPh}_3\}_3](\text{TfO})_3$ (3)	18.38 (s)	16.53 (dd) [761.7], [662]
$[\text{Ag}(\text{OTf})\text{PPh}_2\text{Me}]$		-3.13 (br)
$[\text{N}_3\text{P}_3(\text{NHCy})_6\{\text{AgPPh}_2\text{Me}\}_2](\text{TfO})_2$ (4)	16.22 (br)	-1.90 (dd) [757.6], [651.4]
$[\text{N}_3\text{P}_3(\text{NHCy})_6\{\text{AgPPh}_2\text{Me}\}_3](\text{TfO})_3$ (5)	18.57 (s)	-2.78 (d, br) [718]
$[\text{Ag}(\text{OTf})\text{TPA}]$		-85.82 (br)
$[\text{N}_3\text{P}_3(\text{NHCy})_6\{\text{AgTPA}\}_3](\text{TfO})_3$ (6)	15.93 (s)	-85.46 (br)

^aData taken at RT in CDCl_3 , except for **6** and $[\text{Ag}(\text{OTf})\text{TPA}]$, whose data are in DMSO. Values in parts per million. ^bValues in hertz.

from the peak of the parent phosphazene, is shown by the phosphazene phosphorus atoms in all complexes **2–6**. This downfield shift can be ascribed to deshielding by the silver ion coordinated to the adjacent nitrogen atoms, which increases with the number of metals linked to the adjacent nitrogen atoms. This shift has also been observed in other metallophosphazenes in which metals (such as silver or lithium) are coordinated to the backbone nitrogen atoms.^{23b,c} The signal observed at RT is a single peak even for **2** and **4**, for which a AX_2 spin system corresponding to two types of phosphorus atoms would be expected. This is attributable to a fluxional process, which is typical in the coordination chemistry of silver and can be attributed to exchange phenomena involving all of the phosphazene nitrogen atoms. The fluxionality can be

quenched at low temperature. Thus, the single broad peak observed for the phosphazene phosphorus atoms in **2** and **4** at RT is split into two signals at $-80\text{ }^{\circ}\text{C}$ (as shown in Figure 3 for

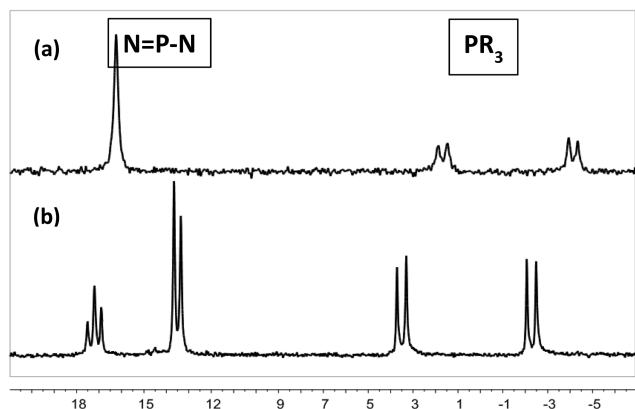


Figure 3. $^{31}\text{P}\{^1\text{H}\}$ NMR spectra of compound **4** in $(\text{CD}_3)_2\text{CO}$ at (a) RT and (b) $-80\text{ }^{\circ}\text{C}$.

4; see also Table 2). The sparingly soluble compound **1** was not fluxional in solution, and two signals were observed for the phosphazene phosphorus atoms in its $^{31}\text{P}\{^1\text{H}\}$ NMR spectrum at RT [10.39 (t, 1P) and 8.43 (d, 2P), AB_2 system, $^2J_{\text{AB}} = 45.1\text{ Hz}$]. Both the poor solubility and nonfluxionality might be associated with the oligomeric or polymeric nature of **1**. However, single crystals suitable for X-ray diffraction analysis could not be obtained.

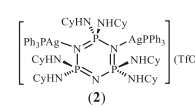
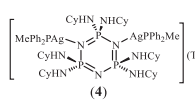
The $^{31}\text{P}\{^1\text{H}\}$ NMR spectra of **2–6** also show signals from the phosphane ligands (see Tables 1 and 2), which are all shifted from those in the starting complexes.^{37,38} For **6**, the phosphane resonates at -85.46 (s) ppm , which is consistent with a silver(I) compound containing TPA acting as a phosphorus-donor ligand.³⁹ Unlike **2–5**, this signal for **6** consists of a broad singlet at RT, and coupling with the two silver isotopomers (^{107}Ag and ^{109}Ag) is not observed, which indicates that the fluxional process in this compound also involves the TPA ligand. The ^1H NMR spectra of **2–6** (see the Experimental Section) also show the signals corresponding to the phosphane ligands and the signals from the cyclohexylamino units (Table 3). These signals, specifically those of NH and NH-CH, were verified by two-dimensional heteronuclear (HSQC ^1H - ^{13}C) correlations. Most significantly, the ^1H NMR spectra of **2–6** all show a unique type of cyclohexylamino unit at RT, as a result of the above-mentioned

fluxional process. For **2** and **4**, though, two types of NHCy units were observed when the spectra were collected at $-80\text{ }^{\circ}\text{C}$, as a consequence of the nonequivalence of all of the amino units. Thus, the single broad peak corresponding to the NH protons, which was observed at $\delta\text{ }4.03\text{ (br, 6H)}$ and 4.0 (br, 6H) for **2** and **4**, respectively, in $(\text{CD}_3)_2\text{CO}$ at RT, was split into two signals at $-80\text{ }^{\circ}\text{C}$ [$\delta\text{ }4.65\text{ (t, 2H)}$ and 4.40 (br, 4H) for **2**; $\delta\text{ }4.55\text{ (br, 2H)}$ and 4.20 (br, 4H) for **4**; see Experimental Section]. As can be observed in Table 3, which presents the ^1H NMR data in CDCl_3 at RT, coordination at phosphazene leads in all complexes to a deshielding of the protons NH, with the rise in the number of metals coordinated to the adjacent nitrogen atoms.

The signals for the phosphazene phosphorus atoms for **7–10** also shift downfield relative to the parent phosphazene in their $^{31}\text{P}\{^1\text{H}\}$ NMR spectra at RT (see Table 4). However, even in **8** and **10** (both with three silver atoms), several signals are observed because of the nongeminal trans configuration of the starting phosphazene **phos-3**, which is expected to be maintained in all metallophosphazenes **7–10**. Thus, the part of the spectrum corresponding to the phosphazene phosphorus atom in the $^{31}\text{P}\{^1\text{H}\}$ NMR spectra at RT shows a single set of resonances of an AB_2 spin system for **10**, with the peaks centered at $\delta\text{ }24.07\text{ (d, 2P)}$ and 23.08 (t, 1P) , $^2J(\text{P-P}) = 33.1\text{ Hz}$, and a broad signal at 24.27 ppm for **8**. For **7** and **9**, this part of the spectrum (between 24 and 19 ppm) is even more complex, as is shown in Figure 4b for **9** as an example, with signals that are broad as a consequence of the above-mentioned fluxional process. In these compounds, **7** and **9**, two diastereomers **A** and **B** are expected (see Chart 2), namely, a pair of $R_{\text{P}_2}, R_{\text{P}_3}$ - or $S_{\text{P}_2}, S_{\text{P}_3}$ -configured enantiomers (**B**) and the diastereomer $R_{\text{P}_1}, R_{\text{P}_2}, S_{\text{P}_3}$ (**A**). At $-80\text{ }^{\circ}\text{C}$, two sets of resonances of two AB_2 spin systems are observed for **9** in this part of the spectrum when the fluxional process is quenched (see Figure 4a), which indicates that both stereoisomers **A** and **B** are present in solution.⁴⁰ The part of the spectrum corresponding to the phosphane ligands (see also Figure 4a) shows two sets of two doublets, consistent with the presence of both diastereomers.⁴¹

In the ^1H NMR spectra of **7–10**, the NH-CH protons resonate as a single broad signal at approximately 2.9 ppm and the NH protons resonate as two broad signals even at RT, as a result of the nonequivalence of all of the amino groups due to the nongeminal trans configuration of the phosphazene ring. The NH protons are also shielded upon coordination. All of these data are collected in the Experimental Section, as are the $^{13}\text{C}\{^1\text{H}\}$ NMR, MS, and microanalytical data. It is worth

Table 2. $^{31}\text{P}\{^1\text{H}\}$ NMR Spectroscopic Data for **2** and **4** at RT and $-80\text{ }^{\circ}\text{C}$

COMPOUND	Spin system	T	$\delta[\text{N-P-Nag}]^a$ $[^2J(\text{P-P})]^b$	$\delta[\text{AgN-P-Nag}]^a$	$\delta[\text{PR}_3]^a$ $[^1J(^{109}\text{Ag-P})]^b$ $[^1J(^{107}\text{Ag-P})]^b$
 (2)	AX ₂	RT	16.11 (br)		17.48 (dd) [748.9], [652.6]
		$-80\text{ }^{\circ}\text{C}$	13.23 (d) [36.3]	17.54 (t)	17.51 (dd) [740.6], [641.3]
 (4)	AX ₂	RT	16.24 (br)		-1.25 (dd) [757.8], [653.5]
		$-80\text{ }^{\circ}\text{C}$	13.50 (d) [36.9]	17.20 (t)	0.64 (dd) [753.9], [652.4]

^aData taken in $(\text{CD}_3)_2\text{CO}$. Values in parts per million. ^bValues in hertz.

Table 3. ^1H NMR Spectroscopic Data for phos-1 and Complexes 2–6^a

compound	$\delta[\text{NH}]$	$\delta[\text{NH}-\text{CH}]$	$\delta[\text{NH}(\text{C}_6\text{H}_{11})]$	$\delta[\text{PPR}_3]$
$[\text{N}_3\text{P}_3(\text{NHCy})_6]$ (phos-1)	2.0 (br, 6H)	3.05 (m, 6H)	1.94, 1.65, 1.50, 1.26, 1.10 (m, 60H)	
$[\text{N}_3\text{P}_3(\text{NHCy})_6\{\text{AgPPh}_3\}_2](\text{TfO})_2$ (2)	3.20 (br, 6H)	3.0 (br, 6H)	1.90, 1.87, 1.66, 1.54, 1.40, 1.26–1.07 (m, 60H)	7.54–7.40 (m, 30H; Ph)
$[\text{N}_3\text{P}_3(\text{NHCy})_6\{\text{AgPPh}_3\}_3](\text{TfO})_3$ (3)	4.20 (br, 6H)	3.02 (br, 6H)	1.86, 1.46, 1.34, 1.25, 1.04–0.85 (m, 60H)	7.49–7.42 (m, 45H; Ph)
$[\text{N}_3\text{P}_3(\text{NHCy})_6\{\text{AgPPh}_2\text{Me}\}_2](\text{TfO})_2$ (4)	3.5 (br, 6H)	2.95 (br, 6H)	1.85, 1.59, 1.42, 1.21, 1.06 (m, 60H)	7.60–7.41 (m, 20H; Ph) 2.11 (d, 6H, $^2J_{\text{P-H}} = 5.9$ Hz; Me)
$[\text{N}_3\text{P}_3(\text{NHCy})_6\{\text{AgPPh}_2\text{Me}\}_3](\text{TfO})_3$ (5)	4.27 (br, 6H)	2.96 (br, 6H)	1.85, 1.50, 1.39, 1.24, 1.06–0.88 (m, 60H)	7.58–7.44 (m, 30H; Ph) 2.11 (d, 9H, $^2J_{\text{P-H}} = 7.6$ Hz; Me)
$[\text{N}_3\text{P}_3(\text{NHCy})_6\{\text{AgTPA}\}_3](\text{TfO})_3$ (6)	3.41 (br, 6H)	2.86 (br, 6H)	1.85, 1.65, 1.53, 1.15 (m, 60H)	4.59 (d), 4.42 (d) (AB system, 18H, $^2J_{\text{H-H}} = 12.6$ Hz; NCH_2N), 4.24 (br, 18H; PCH_2N)

^aData taken at RT in CDCl_3 , except for 6, whose data are in DMSO. Values in parts per million.

Table 4. $^{31}\text{P}\{^1\text{H}\}$ NMR Spectroscopic Data for 7–10 and Starting Products^a

compound	$\delta[\text{N}-\text{P}-\text{N}]^a$ [$^2J(\text{P}-\text{P})]^b$	$\delta[\text{PR}_3]^a$ [$^1J(^{109}\text{Ag}-\text{P})$], b [$^1J(^{107}\text{Ag}-\text{P})$] ^b
$[\text{N}_3\text{P}_3(\text{NHCy})_3(\text{NMe}_2)_3]$ (phos-3)	20.96, 20.70 [44.3]	
$[\text{Ag}(\text{OTf})\text{PPh}_3]$		16.79 (br)
$[\text{N}_3\text{P}_3(\text{NHCy})_3(\text{NMe}_2)_3\{\text{AgPPh}_3\}_2](\text{TfO})_2$ (7)	24.20 (d, 2P), 23.0 (t, 1P) [36.2]	16.58 (dm) [671.5]
$[\text{N}_3\text{P}_3(\text{NHCy})_3(\text{NMe}_2)_3\{\text{AgPPh}_3\}_3](\text{TfO})_3$ (8)	24.27 (br)	16.19 (br)
$[\text{Ag}(\text{OTf})\text{PPh}_2\text{Me}]$		−3.13 (br)
$[\text{N}_3\text{P}_3(\text{NHCy})_3(\text{NMe}_2)_3\{\text{AgPPh}_2\text{Me}\}_2](\text{TfO})_2$ (9)	23.55 (d, br, 2P), 21.05 (t, br, 1P) [40]	−2.13 (dd) [765.0], [665.2]
$[\text{N}_3\text{P}_3(\text{NHCy})_3(\text{NMe}_2)_3\{\text{AgPPh}_2\text{Me}\}_3](\text{TfO})_3$ (10)	24.07 (d, 2P), 23.08 (t, 1P) [33.1]	−3.10 (br)

^aData taken at RT in CDCl_3 . Values in parts per million. ^bValues in hertz.

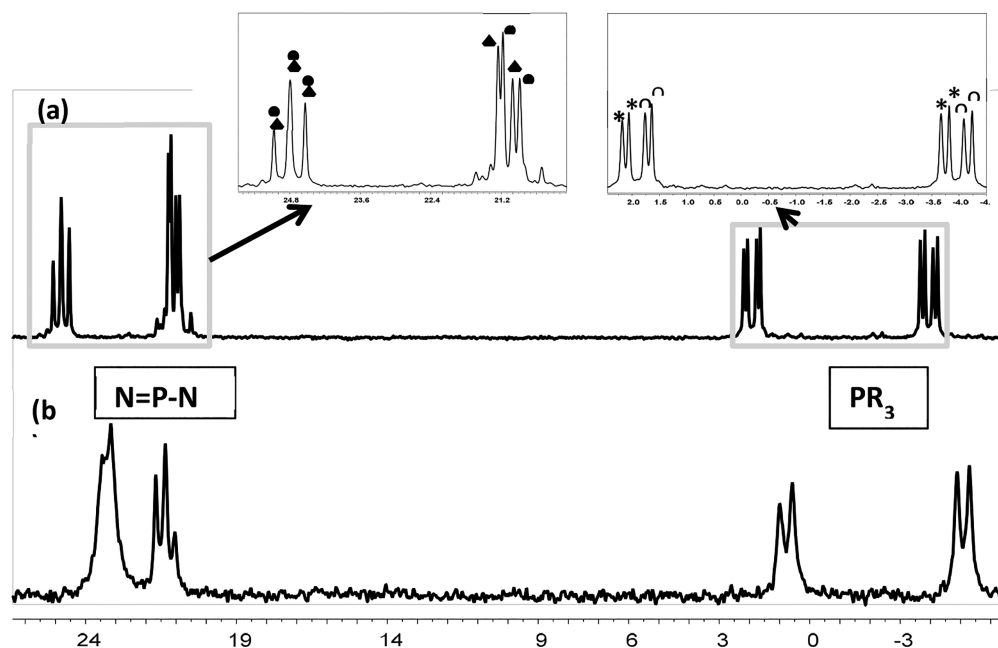


Figure 4. $^{31}\text{P}\{^1\text{H}\}$ NMR spectra of compound 9 in CD_2Cl_2 at (a) -80°C and (b) RT.

noting that the molecular cations of almost all complexes 2–10 are observed in the MS spectra.

The single-crystal X-ray diffraction analyses of the racemic complexes 7 and 9 show that in both cases the $R_{\text{P}_2}, R_{\text{P}_3}$ -configured (and $S_{\text{P}_2}, S_{\text{P}_3}$ -configured) diastereomer is present (see Figures 6 and 7). Single crystals of 5, $7 \cdot 2\text{CH}_2\text{Cl}_2$, and $9 \cdot 1/2\text{C}_6\text{H}_{14}$ were grown by the slow diffusion of hexane into a solution of the complex in dichloromethane. The X-ray analysis confirmed not only the presence of ionic trifluoromethanesulfonate but also the coordination of metals to the ring nitrogen atoms (see Figures 5–7). In the case of 5, the

structure was only confirmed qualitatively but could not be refined satisfactorily because of severely disordered anions and unidentified solvent regions. Selected bond lengths and angles and details of the data collection and refinement for 7 and 9 are given in tables in the Supporting Information. In both compounds 7 and 9, the silver atoms show a nearly linear coordination with angles close to 180° [$167.97(8)$ and $165.57(8)^\circ$ for 7; $168.26(4)$ and $177.26(4)^\circ$ for 9]. The Ag–N and Ag–P bond lengths are typical.^{23g,24a,37a,42} There are also short Ag...O contacts: for 7, Ag2...O1 2.704(4) Å; for 9, Ag1...O1 2.781(2) Å and Ag2...O5 2.870(3) Å. Metalation

Chart 2. Diastereomers Expected for Compounds 7 and 9

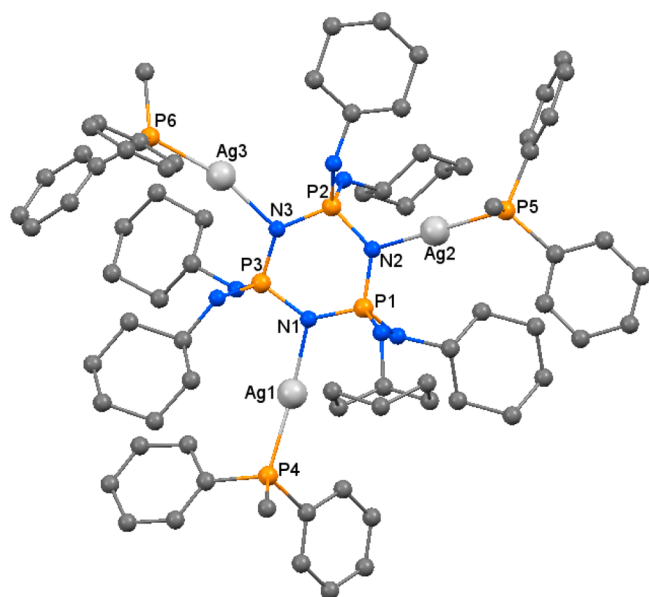
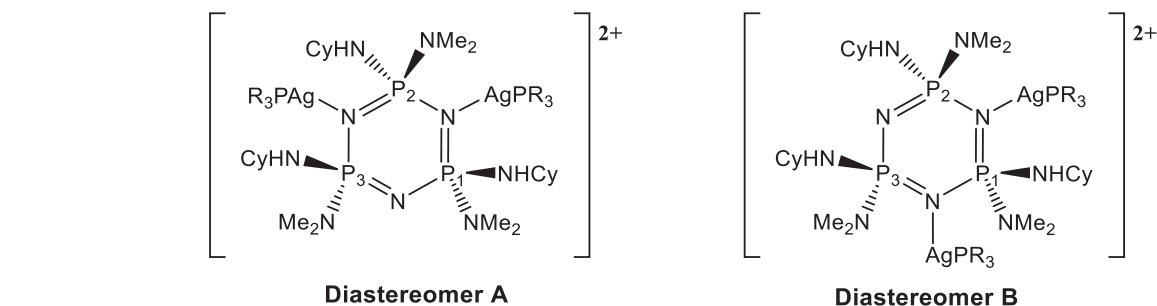


Figure 5. Molecular structure of complex **5** determined by single-crystal X-ray diffraction. Hydrogen atoms, anions, and solvent molecules have been omitted for clarity. The radii are arbitrary.

causes distortion of the cyclophosphazene ring skeleton. The P–N(ring) bonds associated with metal coordination are longer [av. 1.627(3) Å for **7** and 1.6270(15) Å for **9**] than the

P–N(ring) bonds at the noncoordinating nitrogen center [av. 1.583(3) Å for **7** and 1.5861(15) Å for **9**] and also the P–N(ring) bond in the starting phosphazene **phos-1** (1.598 Å).^{28,43} Such an N–P bond length increase flanking the site of coordination (or protonation or alkylation) is known from studies on CPZs.^{23g,24a,44,45} This is consistent with the bonding model of Craig and Paddock.⁴⁶ Accordingly, in such situations, the lone pair on the ring nitrogen atom of the cyclophosphazenes is not available for π -bonding interactions within the ring, causing an increase in the affected bond distance. The exocyclic P–N bond lengths [av. 1.632(3) Å for P–NHCy and 1.649(3) Å for P–NMe₂ in **7**; 1.6341(16) Å for P–NHCy and 1.6530(16) Å for P–NMe₂ in **9**] are longer than the P–N(ring) bond lengths but are shorter than the ideal P–N single-bond value of 1.77 Å.^{27,30c} While the phosphazene rings of the free ligands, i.e., **phos-1**, are planar or close to planarity,⁴³ the coordination to silver causes the rings to pucker, which is evident from the ring torsion angles [maximum absolute values of 24.5(3)° in **7** and 32.9(1)° in **9**].

The NH groups of the ligands form classical hydrogen bonds to the triflate anions: for **7**, N4...O1 2.964(4) Å, N6...O4 2.968(4) Å, and N8...O2 3.135(5) Å; for **9**, N4...O4 2.991(3) Å, N6...O2 3.020(2) Å, and N8...O4 3.374(3) Å.

2.3. Biological Evaluation: Cytotoxic and Antibacterial Activity. All of the complexes are insoluble in water but soluble in DMSO and in the DMSO/water mixtures used in the biological tests (cytotoxic and antibacterial ones). In the cytotoxicity tests, the mixtures used contain a minimal amount

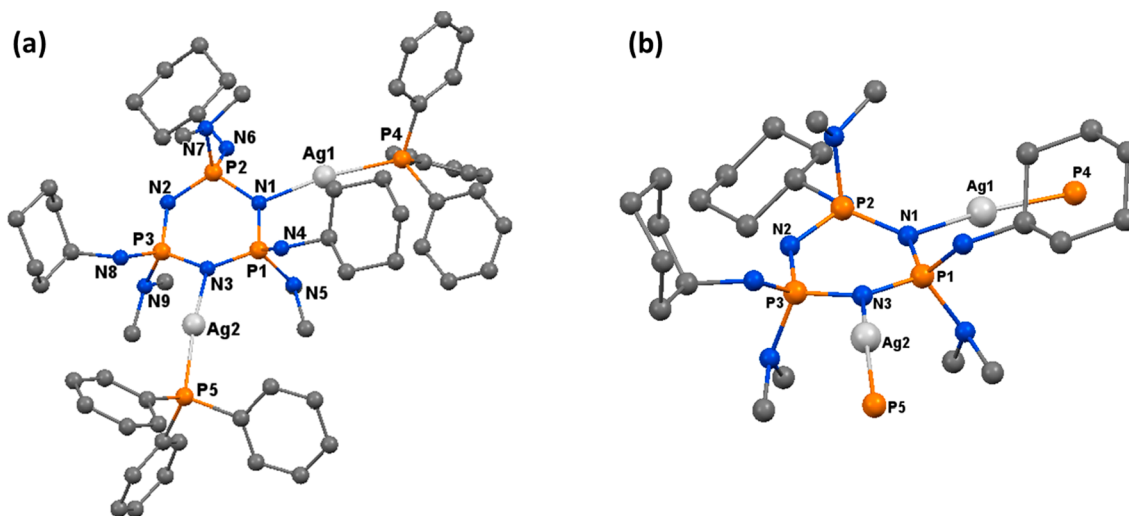


Figure 6. Molecular structure of complex **7** determined by single-crystal X-ray diffraction. Hydrogen atoms, anions, and solvent molecules have been omitted for clarity. The radii are arbitrary.

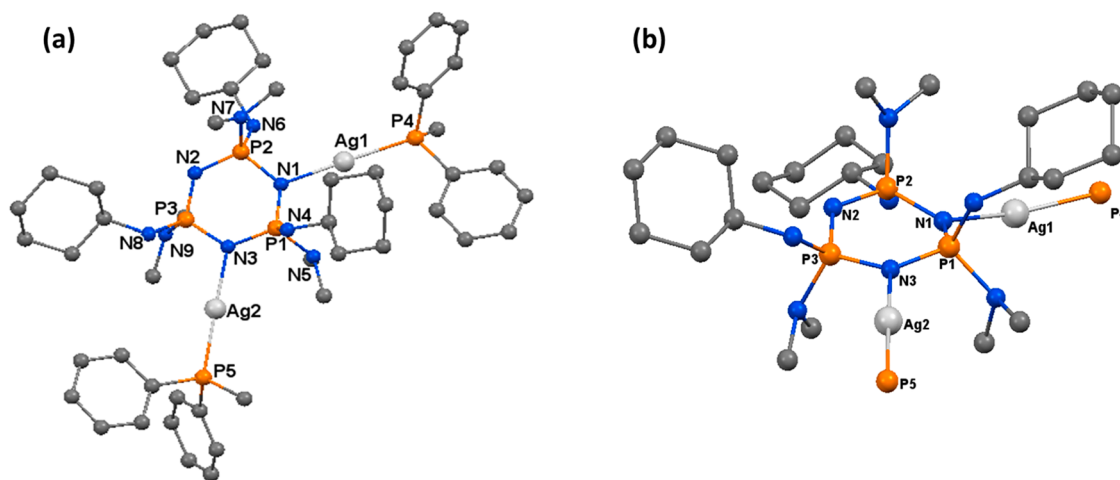


Figure 7. Molecular structure of complex **9** determined by single-crystal X-ray diffraction. Hydrogen atoms, anions, and solvent molecules have been omitted for clarity. The radii are arbitrary.

Table 5. IC₅₀ Obtained by AB and NRU in (a) MCF7 and (b) HepG2 Cell Lines Exposed to the New Metallophosphazenes and Their Precursors after 48 h^a

compound	IC ₅₀ (μM)	
	AB	NRU
(a) MCF7		
N ₃ P ₃ (NHCy) ₆ (phos-1)	14.80 ± 6.10	>25
[N ₃ P ₃ (NHCy) ₆ {Ag(PPh ₃) ₂ }] ₂ (TfO) ₂ (2)	2.87 ± 0.15	2.34 ± 0.28
[N ₃ P ₃ (NHCy) ₆ {Ag(PPh ₃) ₃ }] ₂ (TfO) ₃ (3)	1.60 ± 0.05	2.14 ± 0.65
[Ag(OTf)PPh ₃]	5.67 ± 0.57	8.09 ± 1.39
[N ₃ P ₃ (NHCy) ₆ {Ag(PPh ₂ Me) ₂ }] ₂ (TfO) ₂ (4)	4.89 ± 1.08	2.45 ± 0.66
[N ₃ P ₃ (NHCy) ₆ {Ag(PPh ₂ Me) ₃ }] ₂ (TfO) ₃ (5)	3.88 ± 0.11	3.64 ± 0.05
[Ag(OTf)PPh ₂ Me]	11.76 ± 2.88	14.02 ± 1.05
[N ₃ P ₃ (NHCy) ₆ {Ag(TPA) ₃ }] ₂ (TfO) ₃ (6)	4.46 ± 0.01	3.32 ± 0.12
[Ag(OTf)TPA]	59.93 ± 11.36	30.74 ± 3.06
N ₃ P ₃ (NMe ₂) ₃ (NHCy) ₃ (phos-3)	16.58 ± 4.76	7.81 ± 0.02
[N ₃ P ₃ (NMe ₂) ₃ (NHCy) ₃ {Ag(PPh ₂ Me) ₂ }] ₂ (TfO) ₂ (9)	5.48 ± 0.18	5.95 ± 0.49
[N ₃ P ₃ (NMe ₂) ₃ (NHCy) ₃ {Ag(PPh ₂ Me) ₃ }] ₂ (TfO) ₃ (10)	4.18 ± 0.18	3.44 ± 0.10
cisplatin	56.82 ± 4.23	23.71 ± 1.24
(b) HepG2		
N ₃ P ₃ (NHCy) ₆ (phos-1)	>25	>25
[N ₃ P ₃ (NHCy) ₆ {Ag(PPh ₃) ₂ }] ₂ (TfO) ₂ (2)	1.40 ± 0.23	2.41 ± 0.18
[N ₃ P ₃ (NHCy) ₆ {Ag(PPh ₃) ₃ }] ₂ (TfO) ₃ (3)	0.93 ± 0.37	1.37 ± 0.55
[Ag(OTf)PPh ₃]	4.45 ± 0.37	7.69 ± 1.96
[N ₃ P ₃ (NHCy) ₆ {Ag(PPh ₂ Me) ₂ }] ₂ (TfO) ₂ (4)	2.38 ± 0.12	2.61 ± 0.43
[N ₃ P ₃ (NHCy) ₆ {Ag(PPh ₂ Me) ₃ }] ₂ (TfO) ₃ (5)	2.16 ± 0.13	2.63 ± 0.39
[Ag(OTf)PPh ₂ Me]	11.02 ± 0.09	14.03 ± 1.04
[N ₃ P ₃ (NHCy) ₆ {Ag(TPA) ₃ }] ₂ (TfO) ₃ (6)	2.02 ± 0.34	5.48 ± 0.23
[Ag(OTf)TPA]	45.88 ± 3.34	29.31 ± 4.09
N ₃ P ₃ (NMe ₂) ₃ (NHCy) ₃ (phos-3)	8.80 ± 0.69	10.25 ± 2.05
[N ₃ P ₃ (NMe ₂) ₃ (NHCy) ₃ {Ag(PPh ₂ Me) ₂ }] ₂ (TfO) ₂ (9)	2.82 ± 0.20	4.05 ± 0.24
[N ₃ P ₃ (NMe ₂) ₃ (NHCy) ₃ {Ag(PPh ₂ Me) ₃ }] ₂ (TfO) ₃ (10)	2.76 ± 0.22	3.20 ± 0.24
cisplatin	11.32 ± 1.11	6.94 ± 0.72

^aAll the compounds analyzed were dissolved in DMSO, not exceeding 0.1%, except cisplatin, which was dissolved in water.

of DMSO (≤0.1%). In the antibacterial tests, the solvent DMSO was also used as a control (in the same percentage used to dissolve the compounds) so as to confirm that it did not inhibit bacterial growth. While the tests were performed, no precipitation of any compound at the concentration ranges assayed was observed. The colorless DMSO solutions were very stable at RT. The stability of compounds in DMSO was provided by ³¹P and ¹H NMR spectroscopy. In the Supporting

Information, we have included these spectra for compound **2**, as an example, measured over 48 h, which is the time for the biological assays. These spectra showed the expected signals according to the proposed structure for compound **2**, slightly displaced with respect to those observed for the same complex in other solvents such as acetone, which remain exactly the same for more than 48 h. Among the new metallophosphazenes **1–10**, we have selected **2–6**, **9**, and **10** to carry out the

Table 6. MICs (μM) Obtained for Silver Phosphazenes and Their Precursors against Gram-Positive, Gram-Negative, and MTBC Strains

compound	<i>S. aureus</i> (Gram-positive)	<i>E. coli</i> (Gram-negative)	<i>P. aeruginosa</i> (Gram-negative)	<i>M. bovis</i> BCG	<i>M. tuberculosis</i> H37Rv
$[\text{N}_3\text{P}_3(\text{NHCy})_6]$ (phos-1)	250	125	125	62.5	31.25
$[\text{N}_3\text{P}_3(\text{NHCy})_6\{\text{AgPPh}_3\}_2](\text{TfO})_2$ (2)	≤ 0.12	0.49	3.9	7.8	3.9
$[\text{N}_3\text{P}_3(\text{NHCy})_6\{\text{AgPPh}_3\}_3](\text{TfO})_3$ (3)	0.24	0.97	15.6	≤ 0.12	0.97
$[\text{Ag}(\text{OTf})\text{PPh}_3]$	0.97	3.9	15.6	15.6	31.25
$[\text{N}_3\text{P}_3(\text{NHCy})_6\{\text{AgPPh}_2\text{Me}\}_2](\text{TfO})_2$ (4)	1.95	1.95	7.8	7.8	3.9
$[\text{N}_3\text{P}_3(\text{NHCy})_6\{\text{AgPPh}_2\text{Me}\}_3](\text{TfO})_3$ (5)	0.97	0.97	3.9	3.9	3.9
$[\text{Ag}(\text{OTf})\text{PPh}_2\text{Me}]$	7.8	3.9	15.6	15.6	31.25
$[\text{N}_3\text{P}_3(\text{NHCy})_6\{\text{AgTPA}\}_3](\text{TfO})_3$ (6)	3.9	1.95	3.9	7.8	3.9
$[\text{Ag}(\text{OTf})\text{TPA}]$	250	62.5	250	15.6	31.25
$[\text{N}_3\text{P}_3(\text{NHCy})_3(\text{NMe}_2)_3]$ (phos-3)	62.5	125	125	15.6	15.6
$[\text{N}_3\text{P}_3(\text{NHCy})_3(\text{NMe}_2)_3\{\text{AgPPh}_2\text{Me}\}_2](\text{TfO})_2$ (9)	7.8	3.9	15.6	≤ 0.12	3.9
$[\text{N}_3\text{P}_3(\text{NHCy})_3(\text{NMe}_2)_3\{\text{AgPPh}_2\text{Me}\}_3](\text{TfO})_3$ (10)	7.8	1.95	15.6	≤ 0.12	3.9
AgNO_3^a	31.25	15.6	15.6	15.6	31.25
AgSD	44.8 ^b	22.4 ^b	13–90 ^c	nd ^d	nd ^d

^aData measured by us, under the same conditions as those for the other compounds. ^bData taken from ref 60. ^cData taken from ref 61, where authors studied several strains of *P. aeruginosa*. MICs were transformed by us from milligrams per milliliter to micromolars. ^dNot determined.

biological studies so as to evaluate the structure–activity relationship. Under the same conditions, cisplatin and silver(I) nitrate, two well-known chemotherapeutic and antimicrobial drugs, respectively, have been tested and compared to all of the compounds studied.

Cytotoxic Activity. The in vitro cytotoxicity of the new complexes **2–6**, **9**, and **10** and their precursors (the phosphazene ligands **phos1** and **phos3** and the silver starting complexes) has been evaluated against two tumor human cell lines, MCF7 and HepG2, by two different biomarkers, Alamar Blue (AB) and Neutral Red Uptake (NRU) after 48 h of exposure. At 24 h, the exposed cells were checked under an optical microscope, and the damage was observed at the similar range, which has been calculated after 48 h (see the [Supporting Information](#)). By using both viability assays, median inhibitory concentration (IC_{50}) values ([Table 5a,b](#)) were calculated from the dose–response curves obtained by nonlinear regression analysis. IC_{50} values are the concentrations of a drug required to inhibit tumor cell proliferation by 50% compared to nontreated cells.

All of the tested metallophosphazenes (**2–6**, **9**, and **10**) showed excellent antitumor activities toward the MCF7 cell line with IC_{50} values lower than $5.5 \mu\text{M}$ (see [Table 5a](#)), and the best of these were complexes **2** and **3** with IC_{50} values with both biomarkers lower than $3 \mu\text{M}$. Except $[\text{Ag}(\text{OTf})\text{TPA}]$, all of the compounds that we tested were more cytotoxic than cisplatin toward MCF7. Besides, all of the new metallophosphazenes (**2–6**, **9**, and **10**) were more cytotoxic than their phosphazene ligands and silver precursors and much more cytotoxic than cisplatin, which showed IC_{50} values of 56.82 and $23.71 \mu\text{M}$ in the AB and NRU assays, respectively. In general, NRU proved to be a more sensitive assay for MCF7 cells than AB except for compound **3**, in which both of them are similar.

The cytotoxicity of all metallophosphazenes acquired in HepG2 cells was even more drastic than that in MCF7 ([Table 5b](#)). In the AB assay, the obtained IC_{50} values were lower than $3 \mu\text{M}$, with **2** and **3** being the most cytotoxic compounds, with values of 1.40 and $0.93 \mu\text{M}$, respectively. In this case, in contrast to the results we found for MCF7, the biomarker AB

was more sensitive in comparison to NRU. Once more, all metallophosphazenes showed lower IC_{50} values than their precursors and cisplatin, with values of 11.32 and $6.94 \mu\text{M}$ in the AB and NRU assays, respectively, with the new silver phosphazenes being extraordinarily effective as cytotoxic agents in vitro. Regarding the cytotoxicity of the precursors in the HepG2 cells, only $[\text{Ag}(\text{OTf})\text{PPh}_3]$ was just as or even more cytotoxic than cisplatin but also much less cytotoxic than their silver phosphazenes, **2** and **3**.

As for the structure–activity relationships toward both cell lines in these metallophosphazenes **2–6**, **9**, and **10**, the following can be concluded: (1) the silver atom exerts the cytotoxic activity, which is significantly enhanced by the rise in the number of silver atoms linked to the phosphazene ring (see [Table 5a,b](#); **3** is more toxic than **2**, **5** more than **4**, and **10** more than **9**); (2) the ligands coordinated to the silver atom also have an influence in the cytotoxicity, which is higher in triphenylphosphane derivatives than in those with diphenylmethylphosphane or TPA (see [Table 5a,b](#); **3** is more toxic than **5** or **6**). Moreover, the cytotoxicity was also higher in those with the phosphazene ligand **phos-1** than those with **phos-3** (see [Table 5a,b](#); **4** is more toxic than **9** and **5** more than **10**). Thus, **3** is the most toxic compound, followed by **2**. Remarkably, both metallophosphazenes **2** and **3** were just as toxic as auranofin, a well-known cytotoxic gold(I) compound that is even more toxic than cisplatin for MCF7 and HepG2 cells. The IC_{50} values reported for auranofin are $1.1 \mu\text{M}$ for MCF7 cells⁴⁷ and $2.0 \mu\text{M}$ for HepG2 cells.⁴⁸ The anticancer activity of silver(I) complexes has been summarized in recent reviews,^{2f,9,11c} and the IC_{50} values obtained for all of the tested silver phosphazenes are among the lowest found for any silver derivatives against MCF7 and HepG2 cell lines, taking into account the experimental conditions (measured at 48 h). To the best of our knowledge, the lowest IC_{50} values found in the literature for silver complexes against the mentioned cell lines have been described by Hadjikakou et al. (IC_{50} values range between 1.6 and $2.5 \mu\text{M}$ in MCF7, for acetyl salicylate or hydroxybenzoic acid derivatives),⁴⁹ by Galal et al. (IC_{50} value of $2.0 \mu\text{M}$ in MCF7, for a complex of 2-methyl-1H-benzimidazole-5-carboxylic acid hydrazide),⁵⁰ by Gautier et

al.,⁵¹ Hague et al.,⁵² or Tacke et al.⁵³ (IC_{50} values of $<0.4 \mu M$, $0.9 \mu M$, or ranging from 1.4 to $5.8 \mu M$ in MCF7, respectively, all of them for carbene complexes), by Yilmaz et al. (IC_{50} values ranging from approximately 1 to $5 \mu M$ in MCF7, for saccharinate complexes with mono-⁵⁴ and diphosphane ligands),⁵⁵ by Gimeno et al. (IC_{50} values ranging between 2.81 and $25.42 \mu M$ in MCF7 and HepG2 cells, for complexes with modified amino acid esters and phosphane ligands),⁵⁶ and by McCann, Egan, and co-workers (IC_{50} values between 0.9 and $3.8 \mu M$ in HepG2, for 1,10-phenanthroline-5,6-dione,⁵⁷ 6-hydroxycoumarin-3-carboxylate,⁵⁸ and 4-oxy-3-nitrocoumarin complexes).⁵⁹

Antibacterial Activity. The antibacterial activities of the new complexes **2–6**, **9**, and **10** and their precursors (phosphazene ligands **phos-1** and **phos-3** and silver starting compounds) were tested against Gram-negative strains *E. coli* ATCC 10536 and *P. aeruginosa* ATCC 15442, Gram-positive strain *S. aureus* ATCC 11632, and two MTBC strains, *M. tuberculosis* H37Rv ATCC 27294 and *M. bovis* BCG Pasteur. The minimum inhibitory concentrations (MICs) obtained and those of $AgNO_3$ and silver sulfadiazine (AgSD) are listed in Table 6.

The MIC values of the tested metallophosphazenes (**2–6**, **9**, and **10**) indicated that all of them exhibited excellent antibacterial activity against all bacterial strains used in this work, being much higher than those of $AgNO_3$ and AgSD for the entire range of bacteria studied, except **3**, **9**, and **10**, which had a activity similar to that of $AgNO_3$ against *P. aeruginosa*. The MICs of all metallophosphazenes range from 0.12 to $15.6 \mu M$. All metallophosphazenes exhibited much better activity than their phosphazene ligands and also than their silver precursors except **9** and **10**, which were as effective as their silver precursor $[Ag(OTf)PPh_2Me]$ against *S. aureus*, *E. coli*, and *P. aeruginosa*. **3** also exhibited an activity similar to that of its silver precursor, $[Ag(OTf)PPh_3]$, against *P. aeruginosa*. The phosphazene ligands **phos-1** and **phos-3** were not active against Gram-positive and Gram-negative strains, but they were against the two MTBC strains, *M. tuberculosis* H37Rv and *M. bovis* BCG Pasteur, especially **phos-3**. Moreover, all metallophosphazenes and silver precursors showed better bactericidal properties against *S. aureus* and *E. coli* than against *P. aeruginosa* and, in general, also better than those against the two MTBC strains. The best of these complexes were **2**, **3**, and **5** with MIC values for *S. aureus* and *E. coli* between 0.12 and $0.97 \mu M$ (or 0.2 – $2.2 \mu g/mL$ if the molar mass is taken into account), which are among the lowest values found for any silver derivatives (see ref 2f and references cited therein). **3**, **9**, and **10** also exhibited an outstanding activity against *M. bovis* BCG Pasteur (see Table 6); the MICs for the three complexes are $\leq 0.12 \mu M$ ($0.3 \mu g/mL$ for **3**, $0.2 \mu g/mL$ for **9**, and $0.2 \mu g/mL$ for **11**). **3** also exhibited excellent activity against *M. tuberculosis* H37Rv (see Table 6; $0.97 \mu M$ or $2.2 \mu g/mL$).

As for the structure–activity relationships toward all bacterial strains in these metallophosphazenes, it can be said that the general trends observed for the cytotoxic activity have been followed, in spite of not being so clear in some cases. The following can be concluded: (1) The antibacterial activity is higher in the triphenylphosphane derivatives than those in diphenylmethylphosphane or TPA (see Table 6; **3** is more toxic than **5** or **6**; there is an exception regarding *P. aeruginosa*). (2) The antibacterial activity is also higher in those metallophosphazenes with **phos-1** than in those with **phos-3** (see Table 6; **4** is more toxic than **9** and **5** more than

10; there is an exception regarding *M. bovis* and *M. tuberculosis* H37Rv, which can be attributed to the fact that the free phosphazene ligand **phos-3** was also active against the two MTBC strains). (3) There is not such a clear influence of the number of silver atoms linked to the phosphazene ring as that observed for the cytotoxic activity (see Table 6; **5** is more toxic than **4**, but the activity of **9** and **10** is similar against all bacterial strains used, and **2** is even more toxic than **3** against Gram-positive and Gram-negative strains). Remarkably, as in the case of the cytotoxic properties, both metallophosphazenes **2** and **3** showed outstanding antibacterial activity against all strains studied. The broad spectral antimicrobial efficacy of all of these metallophosphazenes may be explained by the lability of the ligands in these silver(I) complexes. It was concluded that the antimicrobial properties of silver(I) complexes depend upon the fast rate of ligand exchange of the metal ion in the biological system (rather than the solubility, charge, or chirality), which correlates to the nature of the donor atoms coordinated to the silver atom. Weak Ag–O and Ag–N bonds play a key role in determining the wide spectral antibacterial activity of silver(I) complexes because of the easy substitution of the corresponding labile ligands with the sulfur- or nitrogen-donor sites of amino acids or nucleotides in bacteria.⁶²

3. CONCLUSIONS

Two multisite (amino)cyclotriphosphazene ligands, **phos-1** and **phos-3**, were both prepared in high yield ($>80\%$) from $[N_3P_3Cl_6]$ and **phos-2**, respectively. The reaction of **phos-1** or **phos-3** with the silver complexes $[Ag(OTf)L]$ ($OTf = OSO_2CF_3$; $L = PPh_3$, PPh_2Me , or TPA, where $TPA = 1,3,5$ -triazia-7-phosphaadamantane) in dichloromethane and in different molar ratios of 1:2 or 1:3 led to two series of cationic metallophosphazenes, $[N_3P_3(NHCy)_6\{AgL\}_n](TfO)_n$ [$n = 2$, $L = PPh_3$ (**2**), PPh_2Me (**4**); $n = 3$, $L = PPh_3$ (**3**), PPh_2Me (**5**), TPA (**6**)] and *nongem-trans*- $[N_3P_3(NHCy)_3(NMe_2)_3\{AgL\}_n](TfO)_n$ [$n = 2$, $L = PPh_3$ (**7**), PPh_2Me (**9**); $n = 3$, $L = PPh_3$ (**8**), PPh_2Me (**10**)]. In all of them, the silver groups “AgL” are coordinated to the nitrogen atoms of the phosphazene ring, whereby their number (2 or 3) depends on the molar ratio used. This type of coordination was confirmed by NMR spectroscopy and also, more specifically, by single-crystal X-ray diffraction for complexes **5**, **7**, and **9**.

The cytotoxic activity of **2–6**, **9**, and **10** has been studied against two tumor human cell lines, MCF7 (breast adenocarcinoma) and HepG2 (hepatocellular carcinoma). The IC_{50} values, which range from 1.6 to $5.5 \mu M$ for MCF7 and from 0.9 to $2.8 \mu M$ for HepG2, reveal excellent cytotoxic activity for these metal complexes compared with their precursors and much higher than that of cisplatin, with their IC_{50} values being among the lowest found in silver complexes. The structure–activity relationships toward both cell lines were clear. The cytotoxicity is higher in triphenylphosphane derivatives than in those with diphenylmethylphosphane or TPA and is higher in those with the phosphazene ligand **phos-1** than in those with the phosphazene **phos-3**. A significant improvement in the activity was also observed upon a rise in the number of silver atoms linked to the phosphazene ring. The same complexes were also tested against Gram-negative strains *E. coli* and *P. aeruginosa*, Gram-positive strain *S. aureus*, and two MTBC strains, *M. tuberculosis* H37Rv and *M. bovis* BCG Pasteur. The MIC values, which range from 0.12 to $15.6 \mu M$ (some of them being the lowest found in silver complexes), indicated that all of them also exhibited excellent

antibacterial activity against all bacterial strains used, with their activity being much higher than those of AgNO₃ and AgSD. As for the structure–activity relationships, the general trends observed for the cytotoxic activity are also followed for the bacterial growth inhibition of these new metallophosphazenes. Thus, **2** and **3** are the most effective bacterial and cell growth inhibitors, which showed outstanding antitumoral and antibacterial activity against all cell lines and bacterial strains studied. **9** and **10** also exhibited remarkable activity against the two MTBC strains, especially for *M. bovis* BCG Pasteur. The outstanding biological activities of these complexes are worth studying further to determine action mechanisms and to elucidate the possibility of new biological targets.

4. EXPERIMENTAL SECTION

4.1. General Data. IR spectra were recorded in the range 4000–250 cm^{−1} on a PerkinElmer Spectrum-100 (ATR mode) Fourier transform infrared spectrometer. Carbon, hydrogen, nitrogen, and sulfur analyses were performed using a PerkinElmer 240 B microanalyzer. NMR spectra were recorded on a Bruker AV 400 spectrometer. Chemical shifts are quoted relative to SiMe₄ (TMS; ¹H and ¹³C NMR, external) and H₃PO₄ (85%; ³¹P NMR, external) and given in parts per million (ppm). Fast-atom-bombardment (FAB) MS spectra were recorded using a Micromass Autospec spectrometer in positive-ion mode with *m*-nitrobenzyl alcohol as the matrix. Hexachlorocyclotriphosphazene, [N₃P₃Cl₆] (Stream Chemicals), was purified by recrystallization from hot hexane and dried in a vacuum. Metal complexes [Ag(OTf)L] (L = PPh₃, PPh₂Me, or TPA; OTf = OSO₂CF₃) were prepared according to published procedures.^{37a,38,63} The culture medium, fetal bovine serum, and cell culture reagents were obtained from Gibco and Corning (Biomol, Spain). Chemicals for the different assays were provided by VWR International Eurolab and Merck. Plastic materials for the cytotoxicity assays were supplied by Fisher Scientific.

4.2. Synthesis and Spectroscopic Characterization Data.
Synthesis of [N₃P₃(NH₂Cy)₆] (phos-1). To a solution of [N₃P₃Cl₆] (0.348 g, 1 mmol) in dry tetrahydrofuran (20 mL) was added slowly and dropwise a solution of NH₂Cy (4.6 mL, ρ = 0.867 g/mL, 40 mmol) in dry tetrahydrofuran (10 mL). The mixture was stirred at RT for 12 h and then refluxed for 48 h. The precipitate of amine hydrochloride was filtered off, and the solvent was removed from the filtrate in a vacuum. The addition of light petroleum (40–60 °C) led to the precipitation of **phos-1** as a white solid. Successive additions of petroleum ether led to the precipitation of **phos-1** as a white solid.

Yield: 579 mg, 80%. Anal. Calcd for C₃₆H₇₂N₉P₃ (723.94): C, 59.73; H, 10.02; N, 17.41. Found: C, 59.60; H, 9.90; N, 17.32. IR (ATR, cm^{−1}): 3405 (w), 3360 (w), 3224 (w, br) (N–H); 1186 (s, sh), 1178 (vs) (P=N and C–N); 1092 (vs), 1080 (s) (P–NHR). ³¹P{¹H} NMR (CDCl₃): δ 14.44 (s, 3 P; N₃P₃ ring). ¹H NMR (CDCl₃): δ 3.05 (m, 6H; NH–CH), 2.0 (br, 6H; NH), 1.94 (m, 12H; NH(C₆H₁₁)), 1.65 (m, 12H; NH(C₆H₁₁)), 1.50 (m, 6H; NH(C₆H₁₁)), 1.26 (m, 12H; NH(C₆H₁₁)), 1.10 (m, 18H; NH(C₆H₁₁)). ¹H NMR ((CD₃)₂CO): δ 3.03 (m, 6H; NH–CH), 2.36 (br, 6H; NH), 1.97 (m, 12H; NH(C₆H₁₁)), 1.67 (m, 12H; NH(C₆H₁₁)), 1.54 (m, 6H; NH(C₆H₁₁)), 1.28 (m, 12H; NH(C₆H₁₁)), 1.14 (m, 18H; NH(C₆H₁₁)). ¹³C{¹H} NMR ((CD₃)₂CO, APT): δ 50.45 (s, 6C; NH–CH), 36.99, 26.6, 26.17 (s, 30C; CH₂). MS (FAB⁺): *m/z* 725 (100%; [M + H]⁺); and peaks derived from the sequential loss of NH₂Cy and Cy.

Synthesis of nongem-trans-[N₃P₃Cl₃(NMe₂)₃] (phos-2). To a solution of [N₃P₃Cl₆] (3.48 g, 10 mmol) in dry tetrahydrofuran (30 mL) was added slowly and dropwise at 0 °C 60 mmol of NHMe₂ (30 mL of a 2.0 M solution in tetrahydrofuran). The mixture was stirred for 1 h. When the mixture had reached RT, the precipitate of amine hydrochloride was filtered off, and the solvent was removed from the filtrate in a vacuum, affording an oil. The addition of hexane led to the precipitation of **phos-2** as a white solid.

Yield: 3.13 g, 84%. Anal. Calcd for C₆H₁₈Cl₃N₆P₃ (373.53): C, 19.29; H, 4.86; N, 22.50. Found: C, 19.50; H, 4.90; N, 22.40. IR (ATR, cm^{−1}): 1193 (vs), 1172 (vs), 1146 (s, sh) (P=N and C–N); 1059 (m) (P–NR₂); 595 (s), 512 (vs), 495 (vs, br) (P–Cl). ³¹P{¹H} NMR (CDCl₃): δ 28.65 (1P), 28.18 (2P) (AB₂ system, ²J(P–P) = 40.6 Hz; N₃P₃ ring). ¹H NMR (CDCl₃): δ 2.72 (m, N = 17.6 Hz, 6H; N(CH₃)₂), 2.70 (m, N = 18.0 Hz, 12H; N(CH₃)₂). ¹³C{¹H} NMR (CDCl₃): δ 36.40 (s, 2C; N(CH₃)₂), 36.19 (s, 4C; N(CH₃)₂). MS (FAB⁺): *m/z* 373 (100%; [M]⁺); and peaks derived from the sequential loss of NMe₂ and Cl.

Synthesis of nongem-trans-[N₃P₃(NH₂Cy)₃(NMe₂)₃] (phos-3). To a solution of **phos-2** (0.374 g, 1 mmol) in dry tetrahydrofuran (20 mL) was added slowly and dropwise a solution of NH₂Cy (4.6 mL, 40 mmol) in dry tetrahydrofuran (10 mL). The mixture was stirred at RT for 12 h and then refluxed for another 48 h. The precipitate of amine hydrochloride was filtered off, and the solvent was removed from the filtrate in a vacuum. The addition of light petroleum (40–60 °C) led to the precipitation of **phos-3** as a white solid. Successive additions of petroleum ether led to the precipitation of **phos-3** as a white solid.

Yield: 477.4 mg, 85%. Anal. Calcd for C₂₄H₅₄N₉P₃ (561.67): C, 51.32; H, 9.69; N, 22.44. Found: C, 51.30; H, 10.0; N, 22.0. IR (ATR, cm^{−1}): 3418 (w), 3367 (w), 3214 (w, br) (N–H); 1180 (s, sh), 1171 (vs), 1140 (m) (P=N and C–N); 1111 (m, sh), 1096 (s), 1084 (vs) (P–NHR). ³¹P{¹H} NMR (CDCl₃): δ 20.96 (1P), 20.70 (2P) (AB₂ system, ²J(P–P) = 44.3 Hz; N₃P₃ ring). ¹H NMR (CDCl₃): δ 3.01 (br, 3H; NH–CH), 2.62 (m, N = 13.6 Hz, 18H; N(CH₃)₂), 1.96 (m, br, 9H; NH and NH(C₆H₁₁)), 1.64 (br, 6H; NH(C₆H₁₁)), 1.53 (br, 3H; NH(C₆H₁₁)), 1.26 (br, 6H; NH(C₆H₁₁)), 1.09 (br, 9H; NH(C₆H₁₁)). ¹H NMR ((CD₃)₂CO): δ 2.98 (br, 3H; NH–CH), 2.57 (m, N = 14 Hz, 18H; N(CH₃)₂), 2.41 (br, 3H; NH), 1.95 (m, br, 6H; NH(C₆H₁₁)), 1.67 (m, 6H; NH(C₆H₁₁)), 1.54 (m, 3H; NH(C₆H₁₁)), 1.27 (m, 6H; NH(C₆H₁₁)), 1.15 (m, 9H; NH(C₆H₁₁)). ¹³C{¹H} NMR ((CD₃)₂CO, APT): δ 50.38 (d, ²J(P–C) = 10.3 Hz, 2C; NH–CH), 50.28 (d, ²J(P–C) = 10.3 Hz, 1C; NH–CH), 37.60 (s, 6C; N(CH₃)₂), 36.81 (d, ³J(P–C) = 8.4 Hz, 4C; CH₂), 36.73 (d, ³J(P–C) = 11.3 Hz, 2C; CH₂), 26.58, 26.24, 26.17 (s, 9C; CH₂). MS (FAB⁺): *m/z* 562.5 (100%; [M + H]⁺); and peaks derived from the sequential loss of NMe₂ and NH₂Cy.

Synthesis of [N₃P₃(NH₂Cy)₆Ag] (TfO)_n (1). To a solution of **phos-1** (144.8 mg, 0.2 mmol) in acetone (20 mL) was added AgTfO (51.4 mg, 0.2 mmol). The mixture was stirred at RT for 30 min protected from light. The solution was evaporated to ca. 1 mL. The addition of hexane led to the precipitation of **1** as a white solid.

Yield: 129.5 mg, 66%. Anal. Calcd for C₃₇H₇₂AgF₃N₉O₃P₃S (980.88): C, 45.31; H, 7.40; N, 12.85; S, 3.27. Found: C, 45.15; H, 8.01; N, 12.85; S, 3.60. IR (ATR, cm^{−1}): 3308 (m, br) (N–H); 1076 (s) (P–NHR). Other bands: 1297 (s), 1226 (s, br), 1165 (m), 1081 (s), 1030 (vs). ³¹P{¹H} NMR (CDCl₃): δ 10.39 (t, 1P), 8.43 (d, 2P) (AB₂ system, ²J_{AB} = 45.1 Hz; N₃P₃ ring). ¹H NMR (CDCl₃): δ 3.15 (br, 6H; NH), 3.04 (br, 6H; NH–CH), 1.90 (m, 12H; NH(C₆H₁₁)), 1.68 (br, 12H; NH(C₆H₁₁)), 1.56 (m, 6H; NH(C₆H₁₁)), 1.30–1.19 (m, 30H; NH(C₆H₁₁)). ¹⁹F{¹H} NMR (CDCl₃, RT): δ −78.17 (s; SO₂CF₃). MS (FAB⁺): *m/z* 1556 (3%; [(N₃P₃(NH₂Cy)₆]₂Ag]⁺), 831 (3%; [M − SO₂CF₃]⁺), 725 (100%; [M − AgSO₂CF₃ + H]⁺); and peaks derived from the sequential loss of NH₂Cy and Cy.

Synthesis of [N₃P₃(NH₂Cy)₆(AgL)₂](TfO)₂ (L = PPh₃ (2), PPh₂Me (4)). To a solution of **phos-1** (72.4 mg, 0.1 mmol) in dichloromethane (15 mL) was added [Ag(OTf)L] (0.2 mmol, 103.8 mg for **2** or 91.4 mg for **4**), and the mixture was stirred at RT for 30 min protected from light. The solution was evaporated to ca. 1 mL. The addition of hexane led to the precipitation of **2** or **4** as a white solid.

Compound 2. Yield: 130.4 mg, 74%. Anal. Calcd for C₇₄H₁₀₂Ag₂F₆N₉O₆P₃S₂ (1762.39): C, 50.43; H, 5.83; N, 7.15; S, 3.64. Found: C, 50.00; H, 5.30; N, 6.95; S, 3.60. IR (ATR, cm^{−1}): 3285 (m, br) (N–H); 1074 (s) (P–NHR). Other bands: 1284 (m), 1237 (s), 1221 (vs), 1157 (m), 1095 (s), 1025 (vs). ³¹P{¹H} NMR (CDCl₃, RT): δ 16.90 (br s, 3P; N₃P₃ ring), 17.12 (dd, ¹J(¹⁰⁹Ag–P) = 746.1 Hz, ¹J(¹⁰⁷Ag–P) = 653.4 Hz, 2P; PPh₃). ³¹P{¹H} NMR ((CD₃)₂CO, RT): δ 16.11 (br s, 3P; N₃P₃ ring), 17.48 (dd, ¹J(¹⁰⁹Ag–

P) = 748.9 Hz, $^1J(^{107}\text{Ag}-\text{P}) = 652.6$ Hz, 2P; PPh_3). $^{31}\text{P}\{^1\text{H}\}$ NMR ($(\text{CD}_3)_2\text{CO}$, -80°C): δ 17.54 (t, 1P), 13.23 (d, 2P) (AB_2 system, $^2J(\text{P}-\text{P}) = 36.3$ Hz, N_3P_3 ring), 17.51 (dd, $^1J(^{109}\text{Ag}-\text{P}) = 740.6$ Hz, $^1J(^{107}\text{Ag}-\text{P}) = 641.3$ Hz, 2P; PPh_3). ^1H NMR (CDCl_3 , RT): δ 7.54–7.40 (m, 30H; C_6H_5), 3.40 (br, 6H; NH), 3.00 (br, 6H; NH–CH), 1.90 (br, 12H; $\text{NH}(\text{C}_6\text{H}_{11})$), 1.66 (br, 12H; $\text{NH}(\text{C}_6\text{H}_{11})$), 1.54 (br, 6H; $\text{NH}(\text{C}_6\text{H}_{11})$), 1.26–1.09 (m, br, 30H; $\text{NH}(\text{C}_6\text{H}_{11})$). ^1H NMR ($(\text{CD}_3)_2\text{CO}$, RT): δ 7.67–7.54 (m, 30H; C_6H_5), 4.03 (br, 6H; NH), 3.20 (br, 6H; NH–CH), 2.00 (br, 12H; $\text{NH}(\text{C}_6\text{H}_{11})$), 1.63 (br, 12H; $\text{NH}(\text{C}_6\text{H}_{11})$), 1.49 (br, 6H; $\text{NH}(\text{C}_6\text{H}_{11})$), 1.31 (m, br, 12H; $\text{NH}(\text{C}_6\text{H}_{11})$), 1.11 (m, br, 18H; $\text{NH}(\text{C}_6\text{H}_{11})$). ^1H NMR ($(\text{CD}_3)_2\text{CO}$, -80°C): δ 7.72–7.55 (m, 30H; C_6H_5), 4.65 (t, br, 2H; NH), 4.40 (br, 4H; NH), 3.13 (br, 6H; NH–CH), 2.00 (br, 12H; $\text{NH}(\text{C}_6\text{H}_{11})$), 1.65 (br, 6H; $\text{NH}(\text{C}_6\text{H}_{11})$), 1.53–1.41 (br, 12H; $\text{NH}(\text{C}_6\text{H}_{11})$), 1.29–0.56 (m, br, 30H; $\text{NH}(\text{C}_6\text{H}_{11})$). $^{13}\text{C}\{^1\text{H}\}$ NMR ($(\text{CD}_3)_2\text{CO}$, APT, RT): δ 134.96 (d, $^2J(\text{P}-\text{C}) = 16.1$ Hz, 12C; PPh_3), 132.58 (s, 6C; PPh_3), 130.46 (d, $^1J(\text{P}-\text{C}) = 41.9$ Hz, 6C; PPh_3), 130.36 (d, $^3J(\text{P}-\text{C}) = 11.0$ Hz, 12C; PPh_3), 121.99 (q, $^1J(\text{C}-\text{F}) = 321.8$ Hz, 2C; SO_3CF_3), 52.12 (s, 4C; NH–CH), 52.01 (s, 2C; NH–CH), 37.22, 26.14, 26.03 (s, 30C; CH_2). $^{19}\text{F}\{^1\text{H}\}$ NMR (CDCl_3 , RT): δ –77.84 (s; SO_3CF_3). MS (FAB^+): m/z 1613 (100%; $[\text{M} - \text{SO}_3\text{CF}_3]^+$), 1464 (3%; $[\text{M} + \text{H} - 2\text{SO}_3\text{CF}_3]^+$), 1202 (8%; $[\text{M} + \text{H} - 2\text{SO}_3\text{CF}_3 - \text{PPh}_3]^+$), 1093 (30%; $[\text{M} - 2\text{SO}_3\text{CF}_3 - \text{PPh}_3 - \text{Ag}]^+$), 831 (7%; $[\text{M} - 2\text{SO}_3\text{CF}_3 - 2\text{PPh}_3 - \text{Ag}]^+$), 724 (100%; $[\text{M} - 2\text{SO}_3\text{CF}_3 - 2\text{PPh}_3 - 2\text{Ag}]^+$); and peaks derived from the sequential loss of NH_2Cy .

Compound 4. Yield: 142.5 mg, 87%. Anal. Calcd for $\text{C}_{64}\text{H}_{98}\text{Ag}_2\text{F}_6\text{N}_9\text{O}_9\text{P}_5\text{S}_2$ (1638.25): C, 46.92; H, 6.03; N, 7.69; S, 3.91. Found: C, 46.45; H, 6.40; N, 7.35; S, 3.70. IR (ATR, cm^{-1}): 3301 (m, br) (N–H); 1075 (vs) (P–NHR). Other bands: 1275 (m), 1239 (s), 1221 (vs), 1155 (s), 1095 (s, sh), 1025 (vs). $^{31}\text{P}\{^1\text{H}\}$ NMR (CDCl_3 , RT): δ 16.22 (br s, 3P; N_3P_3 ring), –1.90 (dd, $^1J(^{109}\text{Ag}-\text{P}) = 757.6$ Hz, $^1J(^{107}\text{Ag}-\text{P}) = 651.4$ Hz, 2P; PPh_2Me). $^{31}\text{P}\{^1\text{H}\}$ NMR ($(\text{CD}_3)_2\text{CO}$, RT): δ 16.24 (br s, 3P; N_3P_3 ring), –1.25 (dd, $^1J(^{109}\text{Ag}-\text{P}) = 757.8$ Hz, $^1J(^{107}\text{Ag}-\text{P}) = 653.5$ Hz, 2P; PPh_2Me). $^{31}\text{P}\{^1\text{H}\}$ NMR ($(\text{CD}_3)_2\text{CO}$, -80°C): δ 17.20 (t, 1P), 13.50 (d, 2P) (AB_2 system, $^2J(\text{P}-\text{P}) = 36.9$ Hz; N_3P_3 ring), 0.64 (dd, $^1J(^{109}\text{Ag}-\text{P}) = 753.9$ Hz, $^1J(^{107}\text{Ag}-\text{P}) = 652.4$ Hz, 2P; PPh_2Me). ^1H NMR (CDCl_3 , RT): δ 7.60–7.41 (m, 20H; PPh_2Me), 3.5 (br s, 6H; NH), 2.95 (br, 6H; NH–CH), 2.11 (d, $^2J(\text{H}-\text{P}) = 7.6$ Hz, 6H; PPh_2Me), 1.85 (m, 12H; $\text{NH}(\text{C}_6\text{H}_{11})$), 1.59 (m, 12H; $\text{NH}(\text{C}_6\text{H}_{11})$), 1.42 (m, 6H; $\text{NH}(\text{C}_6\text{H}_{11})$), 1.21 (m, 12H; $\text{NH}(\text{C}_6\text{H}_{11})$), 1.06 (m, 18H; $\text{NH}(\text{C}_6\text{H}_{11})$). ^1H NMR ($(\text{CD}_3)_2\text{CO}$, RT): δ 7.80–7.51 (m, 20H; PPh_2Me), 4.00 (br, 6H; NH), 3.13 (br, 6H; NH–CH), 2.20 (d, $^2J(\text{H}-\text{P}) = 7.6$ Hz, 6H; PPh_2Me), 1.99 (m, 12H; $\text{NH}(\text{C}_6\text{H}_{11})$), 1.64 (m, 12H; $\text{NH}(\text{C}_6\text{H}_{11})$), 1.48 (m, 6H; $\text{NH}(\text{C}_6\text{H}_{11})$), 1.32 (m, 12H; $\text{NH}(\text{C}_6\text{H}_{11})$), 1.21–1.05 (m, 18H; $\text{NH}(\text{C}_6\text{H}_{11})$). ^1H NMR ($(\text{CD}_3)_2\text{CO}$, -80°C): δ 7.85–7.54 (m, 20H; PPh_2Me), 4.55 (br, 2H; NH), 4.20 (br, 4H; NH), 3.06 (br, 6H; NH–CH), 2.21 (br, 6H; PPh_2Me), 2.12 (br, 6H; $\text{NH}(\text{C}_6\text{H}_{11})$), 1.90 (br, 6H; $\text{NH}(\text{C}_6\text{H}_{11})$), 1.63 (br, 12H; $\text{NH}(\text{C}_6\text{H}_{11})$), 1.51 (br, 6H; $\text{NH}(\text{C}_6\text{H}_{11})$), 1.29–0.66 (m, br, 30H; $\text{NH}(\text{C}_6\text{H}_{11})$). $^{13}\text{C}\{^1\text{H}\}$ NMR ($(\text{CD}_3)_2\text{CO}$, APT, RT): δ 133.63 (d, $^2J(\text{P}-\text{C}) = 15.1$ Hz, 8C; PPh_2Me), 132.70 (d, $^1J(\text{P}-\text{C}) = 40.5$ Hz, 4C; PPh_2Me), 132.20 (s, 4C; PPh_2Me), 130.16 (d, $^3J(\text{P}-\text{C}) = 10.4$ Hz, 8C; PPh_2Me), 122.03 (q, $^1J(\text{C}-\text{F}) = 310.7$ Hz, 2C; SO_3CF_3), 51.96 (s, 6C; NH–CH), 37.13, 26.21, 26.10 (s, 30C; CH_2), 12.94 (d, $^1J(\text{P}-\text{C}) = 23.4$ Hz, 2C; PPh_2CH_3). $^{19}\text{F}\{^1\text{H}\}$ NMR (CDCl_3 , RT): δ –77.77 (s; SO_3CF_3). MS (FAB^+): m/z 1489 (2%; $[\text{M} - \text{SO}_3\text{CF}_3]^+$), 1340 (1%; $[\text{M} + \text{H} - 2\text{SO}_3\text{CF}_3]^+$), 1140 (2%; $[\text{M} + \text{H} - 2\text{SO}_3\text{CF}_3 - \text{PPh}_2\text{Me}]^+$), 1031 (90%; $[\text{M} - 2\text{SO}_3\text{CF}_3 - \text{PPh}_2\text{Me} - \text{Ag}]^+$), 831 (25%; $[\text{M} - 2\text{SO}_3\text{CF}_3 - 2\text{PPh}_2\text{Me} - \text{Ag}]^+$), 725 (100%; $[\text{M} - 2\text{SO}_3\text{CF}_3 - 2\text{PPh}_2\text{Me} - 2\text{Ag} + \text{H}]^+$); and peaks derived from the sequential loss of NH_2Cy .

Synthesis of $[\text{N}_3\text{P}_3(\text{NH}_2\text{Cy})_6(\text{AgL})_3](\text{TfO})_3$ [$\text{L} = \text{PPh}_3$ (3), PPh_2Me (5), TPA (6)]. To a solution of **phos-1** (72.4 mg, 0.1 mmol) in dichloromethane (15 mL) (for 3 or 5) or methanol for 6 was added $[\text{Ag}(\text{OTf})\text{L}]$ (0.3 mmol, 155.7 mg for 3, 137.1 mg for 5, or 124.2 mg for 6), and the mixture was stirred at RT for 30 min protected from light. The solution was evaporated to ca. 1 mL. The

addition of hexane led to the precipitation of 3 or 5 as a white solid. The addition of diethyl ether led to the precipitation of 6.

Compound 3. Yield: 178.0 mg, 78%. Anal. Calcd for $\text{C}_{93}\text{H}_{117}\text{Ag}_3\text{F}_9\text{N}_9\text{O}_9\text{P}_6\text{S}_3$ (2281.61): C, 48.96; H, 5.17; N, 5.53; S, 4.22. Found: C, 49.00; H, 5.35; N, 4.95; S, 4.10. IR (ATR, cm^{-1}): 3267 (m, br) (N–H); 1074 (vs) (P–NHR). Other bands: 1282 (m), 1236 (s), 1219 (s), 1154 (s), 1095 (s, sh), 1023 (vs). $^{31}\text{P}\{^1\text{H}\}$ NMR (CDCl_3 , RT): δ 18.38 (s, 3P; N_3P_3 ring), 16.53 (dd, $^1J(^{109}\text{Ag}-\text{P}) = 761.7$ Hz, $^1J(^{107}\text{Ag}-\text{P}) = 662.0$ Hz, 3P; PPh_3). ^1H NMR (CDCl_3 , RT): δ 7.49–7.42 (m, 45H; C_6H_5), 4.20 (br, 6H; NH), 3.02 (br, 6H; NH–CH), 1.86 (m, 12H; $\text{NH}(\text{C}_6\text{H}_{11})$), 1.46 (m, 12H; $\text{NH}(\text{C}_6\text{H}_{11})$), 1.34 (m, 6H; $\text{NH}(\text{C}_6\text{H}_{11})$), 1.25 (m, 12H; $\text{NH}(\text{C}_6\text{H}_{11})$), 1.04–0.85 (m, 18H; $\text{NH}(\text{C}_6\text{H}_{11})$). $^{13}\text{C}\{^1\text{H}\}$ NMR (CDCl_3 , APT, RT): δ 134.07 (d, $^2J(\text{P}-\text{C}) = 11.0$ Hz, 18C; PPh_3), 131.40 (s, 9C; PPh_3), 130.03 (s, 9C; PPh_3), 129.40 (s, 18C; PPh_3), 120.53 (q, $^1J(\text{C}-\text{F}) = 320.2$ Hz, 3C; SO_3CF_3), 51.89 (s, 6C; NH–CH), 36.60, 25.37, 25.12 (s, 30C; CH_2). $^{19}\text{F}\{^1\text{H}\}$ NMR (CDCl_3 , RT): δ –77.86 (s; SO_3CF_3). MS (FAB^+): m/z 2132 (1%; $[\text{M} - \text{SO}_3\text{CF}_3]^+$), 1613 (3%; $[\text{M} - 2\text{SO}_3\text{CF}_3 - \text{PPh}_3 - \text{Ag}]^+$), 1464 (1%; $[\text{M} - 3\text{SO}_3\text{CF}_3 - \text{PPh}_3 - \text{Ag} + \text{H}]^+$), 1202 (1%; $[\text{M} - 3\text{SO}_3\text{CF}_3 - 2\text{PPh}_3 - \text{Ag} + \text{H}]^+$), 1094 (100%; $[\text{M} - 3\text{SO}_3\text{CF}_3 - 2\text{PPh}_3 - 2\text{Ag}]^+$), 830 (20%; $[\text{M} - 3\text{SO}_3\text{CF}_3 - 3\text{PPh}_3 - 2\text{Ag}]^+$), 725 (35%; $[\text{M} - 3\text{SO}_3\text{CF}_3 - 3\text{PPh}_3 - 3\text{Ag} + \text{H}]^+$); and peaks derived from the sequential loss of NH_2Cy .

Compound 5. Yield: 136.2 mg, 65%. Anal. Calcd for $\text{C}_{78}\text{H}_{111}\text{Ag}_3\text{F}_9\text{N}_9\text{O}_9\text{P}_6\text{S}_3$ (2095.40): C, 44.71; H, 5.34; N, 6.02; S, 4.59. Found: C, 44.45; H, 5.70; N, 5.85; S, 4.40. IR (ATR, cm^{-1}): 3281 (m, br) (N–H); 1076 (vs) (P–NHR). Other bands: 1281 (m), 1239 (s), 1221 (s), 1156 (s), 1096 (m, sh), 1024 (vs). $^{31}\text{P}\{^1\text{H}\}$ NMR (CDCl_3 , RT): δ 18.57 (s, 3P; N_3P_3 ring), –2.78 (d, br, $^1J(\text{Ag}-\text{P}) = 718.0$ Hz, 3P; PPh_2Me). ^1H NMR (CDCl_3 , RT): δ 7.58–7.44 (m, 30H; PPh_2Me), 4.27 (br, 6H; NH), 2.96 (br, 6H; NH–CH), 2.11 (d, $^2J(\text{H}-\text{P}) = 7.6$ Hz, 9H; PPh_2Me), 1.85 (m, 12H; $\text{NH}(\text{C}_6\text{H}_{11})$), 1.50 (m, 12H; $\text{NH}(\text{C}_6\text{H}_{11})$), 1.39 (m, 6H; $\text{NH}(\text{C}_6\text{H}_{11})$), 1.24 (m, 12H; $\text{NH}(\text{C}_6\text{H}_{11})$), 1.06–0.88 (m, 18H; $\text{NH}(\text{C}_6\text{H}_{11})$). ^1H NMR ($(\text{CD}_3)_2\text{CO}$, RT): δ 7.77–7.51 (m, 30H; PPh_2Me), 4.38 (br, 6H; NH), 3.15 (br, 6H; NH–CH), 2.20 (d, $^2J(\text{H}-\text{P}) = 7.6$ Hz, 9H; PPh_2Me), 2.0 (m, 12H; $\text{NH}(\text{C}_6\text{H}_{11})$), 1.61 (m, 12H; $\text{NH}(\text{C}_6\text{H}_{11})$), 1.46 (m, 6H; $\text{NH}(\text{C}_6\text{H}_{11})$), 1.40–1.27 (m, 12H; $\text{NH}(\text{C}_6\text{H}_{11})$), 1.10–1.05 (m, 18H; $\text{NH}(\text{C}_6\text{H}_{11})$). $^{13}\text{C}\{^1\text{H}\}$ NMR ($(\text{CD}_3)_2\text{CO}$, APT, RT): δ 133.56 (d, $^2J(\text{P}-\text{C}) = 15.2$ Hz, 12C; PPh_2Me), 132.79 (d, $^1J(\text{P}-\text{C}) = 39.3$ Hz, 6C; PPh_2Me), 132.16 (s, 6C; PPh_2Me), 130.15 (d, $^3J(\text{P}-\text{C}) = 10.4$ Hz, 12C; PPh_2Me), 121.95 (q, $^1J(\text{C}-\text{F}) = 312.6$ Hz, 3C; SO_3CF_3), 52.35 (s, 6C; NH–CH), 37.28, 26.15, 25.95 (s, 30C; CH_2), 12.95 (d, $^1J(\text{P}-\text{C}) = 23.7$ Hz, 3C; PPh_2CH_3). $^{19}\text{F}\{^1\text{H}\}$ NMR (CDCl_3 , RT): δ –77.87 (s; SO_3CF_3). MS (FAB^+): m/z 1598 (5%; $[\text{M} - 2\text{SO}_3\text{CF}_3 - \text{PPh}_2\text{Me} + \text{H}]^+$), 1031 (5%; $[\text{M} - 3\text{SO}_3\text{CF}_3 - 2\text{PPh}_2\text{Me} - 2\text{Ag}]^+$), 725 (100%; $[\text{M} - 3\text{SO}_3\text{CF}_3 - 3\text{PPh}_2\text{Me} - 3\text{Ag} + \text{H}]^+$); and peaks derived from the sequential loss of NH_2Cy .

Compound 6. Yield: 137.6 mg, 70%. Anal. Calcd for $\text{C}_{57}\text{H}_{108}\text{Ag}_3\text{F}_9\text{N}_8\text{O}_9\text{P}_6\text{S}_3$ (1966.21): C, 34.82; H, 5.54; N, 12.82; S, 4.89. Found: C, 34.35; H, 5.80; N, 12.50; S, 4.55. IR (ATR, cm^{-1}): 3324 (m, br) (N–H); 1080 (m) (P–NHR). Other bands: 1267 (m, sh), 1238 (s), 1221 (s), 1158 (m), 1096 (m), 1026 (vs). $^{31}\text{P}\{^1\text{H}\}$ NMR (DMSO , RT): δ 15.75 (s, 3P; N_3P_3 ring), –85.51 (s, br, 3P; TPA). ^1H NMR (DMSO , RT): δ 4.59, 4.42 (AB system, $^2J(\text{H}-\text{H}) = 12.6$ Hz, 18H; NCH_2N), 4.24 (s, br, 18H; NCH_2P), 3.41 (br, 6H; NH), 2.86 (br, 6H; NH–CH), 1.85 (m, br, 12H; $\text{NH}(\text{C}_6\text{H}_{11})$), 1.65 (m, br, 12H; $\text{NH}(\text{C}_6\text{H}_{11})$), 1.53 (m, br, 6H; $\text{NH}(\text{C}_6\text{H}_{11})$), 1.15 (m, br, 30H; $\text{NH}(\text{C}_6\text{H}_{11})$). $^{19}\text{F}\{^1\text{H}\}$ NMR (DMSO , RT): δ –77.72 (s; SO_3CF_3). MS (MALDI, ditranol): m/z 724 (100%; $[\text{M} - 3\text{SO}_3\text{CF}_3 - 3\text{TPA} - 3\text{Ag} + \text{H}]^+$); and peaks derived from the sequential loss of NH_2Cy .

Synthesis of nongem-trans- $[\text{N}_3\text{P}_3(\text{NH}_2\text{Cy})_3(\text{NMe}_2)_3(\text{AgL})_2](\text{TfO})_2$ [$\text{L} = \text{PPh}_3$ (7), PPh_2Me (9)]. To a solution of **phos-3** (56.1 mg, 0.1 mmol) in dichloromethane (15 mL) was added $[\text{Ag}(\text{OTf})\text{L}]$ (0.2 mmol, 103.8 mg for 7 or 91.4 mg for 9). The mixture was stirred at RT for 30 min protected from light. The solution was evaporated to ca. 1 mL. The addition of hexane led to the precipitation of 7 or 9 as a white solid.

Compound 7. Yield: 100.8 mg, 63%. Anal. Calcd for $C_{62}H_{84}Ag_2F_6N_9O_6P_5S_2$ (1600.12): C, 46.54; H, 5.29; N, 7.88; S, 4.01. Found: C, 46.95; H, 5.45; N, 7.70; S, 4.00. IR (ATR, cm^{-1}): 3283 (m, br) (N–H); 1078 (vs) (P–N). Other bands: 1284 (m), 1237 (s), 1221 (vs), 1157 (m), 1095 (s), 1025 (vs). $^{31}P\{^1H\}$ NMR ($CDCl_3$, RT): δ 24.20 (d, 2P), 23.0 (t, 1P) (AB_2 system, $^2J(P-P) = 36.2$ Hz; N_3P_3 ring), 16.58 (d, br, $^1J(Ag-P) = 671.5$ Hz). 1H NMR ($CDCl_3$, RT): δ 7.51–7.48 (m, 30H; PPh_3), 4.62 (br, 1H; NH), 4.44 (br, 2H; NH), 2.86 (br, 3H; NH–CH), 2.76–2.71 (m, 18H; $N(CH_3)_2$), 1.99–1.85 (m, 6H; $NH(C_6H_{11})$), 1.70 (m, 6H; $NH(C_6H_{11})$), 1.57–1.27 (m, 9H; $NH(C_6H_{11})$), 1.13–0.97 (m, 9H; $NH(C_6H_{11})$). $^{19}F\{^1H\}$ NMR ($CDCl_3$, RT): δ –78.01 (s; SO_3CF_3). MS (FAB $^+$) m/z 1600 (1%; $[M]^+$), 1451 (1%; $[M - SO_3CF_3]^+$), 1302 (1%; $[M - 2SO_3CF_3 + H]^+$), 1189 (1%; $[M - SO_3CF_3 - PPh_3]^+$), 1040 (1%; $[M - 2SO_3CF_3 - PPh_3 + H]^+$), 933 (25; $[M - 2SO_3CF_3 - PPh_3 - Ag]^+$), 562.5 (100%; $[M - 2SO_3CF_3 - 2PPh_3 - 2Ag + H]^+$); and peaks derived from the sequential loss of NMe_2 and $NHCy$.

Compound 9. Yield: 106.3 mg, 72%. Anal. Calcd for $C_{52}H_{80}Ag_2F_6N_9O_6P_5S_2$ (1475.98): C, 42.31; H, 5.46; N, 8.54; S, 4.35. Found: C, 42.73; H, 5.60; N, 8.32; S, 4.16. IR (ATR, cm^{-1}): 3293 (m, br) (N–H); 1077 (s) (P–N). Other bands: 1281 (m), 1235 (s), 1221 (s), 1155 (s), 1100 (m, sh), 1026 (vs). $^{31}P\{^1H\}$ NMR ($CDCl_3$, RT): δ 23.55 (br, 2P), 21.05 (br, 1P), (AB_2 system; N_3P_3 ring), –2.13 (dd, $^1J(^{109}Ag-P) = 765.0$ Hz, $^1J(^{107}Ag-P) = 665.2$ Hz, 2P; PPh_2Me). $^{31}P\{^1H\}$ NMR (CD_2Cl_2 , –80 $^{\circ}C$): δ 24.80 (t, 1P), 21.13 (d, 2P) (AB_2 system, $^2J(P-P) = 30.1$ Hz; N_3P_3 ring); 24.80 (t, 1P), 21.03 (d, 2P), (AB_2 system, $^2J(P-P) = 34.8$ Hz; N_3P_3 ring), –0.81 (dd, $^1J(^{109}Ag-P) = 728.6$ Hz, $^1J(^{107}Ag-P) = 696.0$ Hz, 2P; PPh_2Me), –1.23 (dd, $^1J(^{109}Ag-P) = 728.9$ Hz, $^1J(^{107}Ag-P) = 695.9$ Hz, 2P; PPh_2Me). 1H NMR ($CDCl_3$, RT): δ 7.56–7.41 (m, 20H; PPh_2Me), 4.24 (t, br, $^2J(P-H) = 9.6$ Hz 1H; NH), 4.03 (br, 2H; NH), 2.84 (br, 3H; NH–CH), 2.71–2.66 (m, 18H; $N(CH_3)_2$), 2.11 (d, $^2J(P-H) = 7.6$ Hz, 6H; PPh_2Me), 1.98–1.83 (m, 6H; $NH(C_6H_{11})$), 1.67 (m, 6H; $NH(C_6H_{11})$), 1.50–1.43 (br, 3H; $NH(C_6H_{11})$), 1.36–1.21 (m, 6H; $NH(C_6H_{11})$), 1.13–1.03 (m, 9H; $NH(C_6H_{11})$). 1H NMR (CD_2Cl_2 , –80 $^{\circ}C$): δ 7.61–7.45 (m, 20H; PPh_2Me), 4.31 (m, 2H; NH), 4.02 (t, $^2J(P-H) = 9.0$ Hz, 1H; NH), 2.74 (br, 3H; NH–CH), 2.68–2.56 (m, 18H; $N(CH_3)_2$), 2.07 (d, $^2J(P-H) = 7.2$ Hz, 6H; PPh_2Me), 2.07 (m, 3H; $NH(C_6H_{11})$), 1.60 (m, 6H; $NH(C_6H_{11})$), 1.49 (m, 6H; $NH(C_6H_{11})$), 1.35–0.93 (m, 15H; $NH(C_6H_{11})$). 1H NMR ($(CD_3)_2CO$, RT): δ 7.75–7.52 (m, 20H; PPh_2Me), 4.27 (br, 3H; NH), 3.02 (br, 3H; NH–CH), 2.81 (m, $N = 11.6$ Hz, 18H; $N(CH_3)_2$), 2.20 (d, $^2J(P-H) = 7.2$ Hz, 6H; PPh_2Me), 1.99–1.89 (m, 6H; $NH(C_6H_{11})$), 1.67 (m, 6H; $NH(C_6H_{11})$), 1.54–1.49 (m, 3H; $NH(C_6H_{11})$), 1.37–1.26 (m, 6H; $NH(C_6H_{11})$), 1.24–1.03 (m, 9H; $NH(C_6H_{11})$). $^{13}C\{^1H\}$ NMR ($(CD_3)_2CO$, APT, RT): δ 133.44 (d, $^2J(P-C) = 15.0$ Hz, 8C; PPh_2Me), 132.91 (d, $^1J(P-C) = 38.8$ Hz, 4C; PPh_2Me), 132.10 (s, 4C; PPh_2Me), 130.16 (d, $^3J(P-C) = 10.3$ Hz, 8C; PPh_2Me), 122.10 (q, $^1J(C-F) = 315.8$ Hz, 2C; SO_3CF_3), 51.87 (s, 3C; NH–CH), 38.05 (s, 6C; $N(CH_3)_2$), 37.11 (s, 2C; CH_2), 36.71 (d, $^3J(P-C) = 13.2$ Hz, 4C; CH_2), 26.27, 26.09 (s, 9C; CH_2), 12.72 (d, $^1J(P-C) = 23.0$ Hz, 2C; PPh_2CH_3). $^{19}F\{^1H\}$ NMR ($CDCl_3$, RT): δ –77.88 (s; SO_3CF_3). MS (FAB $^+$): m/z 1327 (1%; $[M - SO_3CF_3]^+$), 1178 (1%; $[M - 2SO_3CF_3 + H]^+$), 1127 (1%; $[M - SO_3CF_3 - PPh_2Me]^+$), 978 (1%; $[M - 2SO_3CF_3 - PPh_2Me + H]^+$), 869 (30%; $[M - 2SO_3CF_3 - PPh_2Me - Ag]^+$), 562 (100% $[M - 2SO_3CF_3 - 2PPh_2Me - 2Ag]^+$); and peaks derived from the sequential loss of NMe_2 and $NHCy$.

Synthesis of nongem-trans- $[N_3P_3(NHCy)_3(NMe_2)_3(Ag)_3](TfO)_3$ [$L = PPh_3$ (8**), PPh_2Me (**10**)].** To a solution of **phos-3** (56.1 mg, 0.1 mmol) in dichloromethane (15 mL) was added $[Ag(OTf)_2L]$ (0.3 mmol, 155.7 mg for **8** or 137.1 mg for **10**). The mixture was stirred at RT for 30 min protected from light. The solution was evaporated to ca. 1 mL. The addition of hexane led to the precipitation of **8** or **10** as a white solid.

Compound 8. Yield: 158.9 mg, 75%. Anal. Calcd for $C_{81}H_{99}Ag_3F_9N_9O_9P_6S_3$ (2119.34): C, 45.90; H, 4.71; N, 5.95; S, 4.54. Found: C, 46.14; H, 5.05; N, 6.23; S, 4.32. IR (ATR, cm^{-1}):

3257 (m, br) (N–H); 1079 (s) (P–N). Other bands: 1282 (m), 1236 (s), 1219 (s), 1154 (s), 1095 (s, sh), 1023 (vs). $^{31}P\{^1H\}$ NMR ($CDCl_3$, RT): δ 24.27 (br, 3P; N_3P_3 ring), 16.19 (br, $^1J(Ag-P) = 671.5$ Hz, 3P; PPh_3). 1H NMR ($CDCl_3$, RT): δ 7.46–7.42 (m, 45H; PPh_3), 4.76 (br, 1H; NH), 4.54 (br, 2H; NH), 2.85 (br, 3H; NH–CH), 2.75 (m, 18H; $N(CH_3)_2$), 2.0–1.84 (m, 6H; $NH(C_6H_{11})$), 1.74 (m, 3H; $NH(C_6H_{11})$), 1.50–1.27 (m, 12H; $NH(C_6H_{11})$), 1.10–0.95 (m, 9H; $NH(C_6H_{11})$). $^{19}F\{^1H\}$ NMR ($CDCl_3$, RT): δ –77.84 (s; SO_3CF_3). MS (FAB $^+$) m/z 1450 (1%; $[M - 2SO_3CF_3 - PPh_3 - Ag]^+$), 1301 (1%; $[M - 3SO_3CF_3 - PPh_3 - Ag + H]^+$), 1188 (1%; $[M - 2SO_3CF_3 - 2PPh_3 - Ag]^+$), 1038 (1%; $[M - 3SO_3CF_3 - 2PPh_3 - Ag + H]^+$), 931 (100%; $[M - 3SO_3CF_3 - 2PPh_3 - 2Ag]^+$), 561 (90%; $[M - 3SO_3CF_3 - 3PPh_3 - 3Ag]^+$); and peaks derived from the sequential loss of NMe_2 and $NHCy$.

Compound 10. Yield: 135.3 mg, 70%. Anal. Calcd for $C_{66}H_{93}Ag_3F_9N_9O_9P_6S_3$ (1933.13): C, 41.01; H, 4.85; N, 6.52; S, 4.98. Found: C, 41.40; H, 5.13; N, 6.96; S, 4.80. IR (ATR, cm^{-1}): 3269 (m, br) (N–H); 1079 (s, br) (P–N). Other bands: 1279 (m), 1237 (s), 1221 (s), 1151 (s), 1095 (s, sh), 1025 (vs). $^{31}P\{^1H\}$ NMR ($CDCl_3$, RT): δ 24.07 (d, 2P), 23.08 (t, 1P) (AB_2 system, $^2J(P-P) = 33.1$ Hz; N_3P_3 ring), –3.10 (br, 3P; PPh_2Me). 1H NMR ($CDCl_3$, RT): δ 7.55–7.41 (m, 30H; PPh_2Me), 4.55 (t, $^2J(P-H) = 10.3$ Hz, 1H; NH), 4.36 (t, br, $^2J(P-H) = 9.3$ Hz, 2H; NH), 2.87 (br, 3H; NH–CH), 2.72 (m, $N = 11.2$ Hz, 18H; $N(CH_3)_2$), 2.09 (d, $^2J(H-P) = 7.6$ Hz, 9H; PPh_2Me), 1.94 (m, 3H; $NH(C_6H_{11})$), 1.82 (m, 3H; $NH(C_6H_{11})$), 1.71 (m, 3H; $NH(C_6H_{11})$), 1.56 (m, 6H; $NH(C_6H_{11})$), 1.43–1.26 (m, 6H; $NH(C_6H_{11})$), 1.12–0.95 (m, 9H; $NH(C_6H_{11})$). 1H NMR ($(CD_3)_2CO$, RT): δ 7.75–7.51 (m, 30H; PPh_2Me), 4.43 (m, 3H; NH), 3.02 (br, 3H; NH–CH), 2.82 (m, $N = 11.6$ Hz, 18H; $N(CH_3)_2$), 2.18 (d, $^2J(H-P) = 7.2$ Hz, 9H; PPh_2Me), 2.00 (m, 3H; $NH(C_6H_{11})$), 1.89 (m, 3H; $NH(C_6H_{11})$), 1.65 (m, 6H; $NH(C_6H_{11})$), 1.50 (m, 3H; $NH(C_6H_{11})$), 1.34 (m, 6H; $NH(C_6H_{11})$), 1.22–1.03 (m, 9H; $NH(C_6H_{11})$). $^{13}C\{^1H\}$ NMR ($(CD_3)_2CO$, APT): δ 133.43 (d, $^2J(P-C) = 15.2$ Hz, 12C; PPh_2Me), 133.05 (s, 6C; PPh_2Me), 131.95 (s, 6C; PPh_2Me), 130.09 (d, $^3J(P-C) = 10.2$ Hz, 12C; PPh_2Me), 122.06 (q, $^1J(C-F) = 321.2$ Hz, 3C; SO_3CF_3), 51.95 (s, 2C; NH–CH), 51.87 (s, 1C; NH–CH), 38.12 (s, 4C; $N(CH_3)_2$), 38.06 (s, 2C; $N(CH_3)_2$), 37.15 (s, 2C; CH_2), 36.68 (d, $^3J(P-C) = 15.5$ Hz, 4C; CH_2), 26.28, 26.09 (s, 9C; CH_2), 12.72 (d, $^1J(P-C) = 26.0$ Hz, 3C; PPh_2CH_3). $^{19}F\{^1H\}$ NMR ($CDCl_3$, RT): δ –77.80 (s; SO_3CF_3). MS (FAB $^+$) m/z 1733 (1%; $[M - PPh_2Me]^+$), 1327 (1%; $[M - 2SO_3CF_3 - PPh_2Me - Ag]^+$), 1178 (1%; $[M - 3SO_3CF_3 - PPh_2Me - Ag + H]^+$), 1127 (1%; $[M - 2SO_3CF_3 - 2PPh_2Me - Ag]^+$), 977 (1%; $[M - 3SO_3CF_3 - 2PPh_2Me - Ag + H]^+$), 869 (40%; $[M - 3SO_3CF_3 - 2PPh_2Me - 2Ag]^+$), 562 (100%; $[M - 3SO_3CF_3 - 3PPh_2Me - 3Ag + H]^+$); and peaks derived from the sequential loss of NMe_2 and $NHCy$.

4.3. X-ray Structure Determinations. Crystals were mounted on glass fibers and transferred to the cold gas stream of a Bruker SMART 1000 CCD diffractometer. Measurements were made at –130 $^{\circ}C$. Absorption corrections were based on multiscans. Structures were refined anisotropically using the program *SHELXL-2017*.⁶⁴ Hydrogen atoms of the NH groups were refined freely but with N–H distance restraints (“SADI”). Methyl groups were refined as idealized rigid groups allowed to rotate but not tip. Other hydrogen atoms were included using a riding model starting from calculated positions. *Special features:* For **7**, two dichloromethane sites were identified and could be refined but were not entirely satisfactory (high U values; significant residual electron density). Attempts to refine disordered models were unsuccessful. Accordingly, the program *SQUEEZE* (part of the *PLATON* suite)⁶⁵ was used to remove mathematically the effects of the solvent. The chemical formula and associated parameters were calculated using an idealized composition of two dichloromethane molecules per asymmetric unit. For **9**, the cyclohexyl group C51–S6 is disordered over two positions. Appropriate restraints were employed to improve the refinement stability, but the dimensions of the disordered groups should be interpreted with caution. The dimensions of the hexane molecule, which lies across an inversion center, are not entirely satisfactory, despite the use of restraints.

CCDC 1946587 and 1946588 contain the supplementary crystallographic data for this paper (for 7 and 9, respectively).

4.4. Cell Cultures. To assess the cellular cytotoxicity and antitumoral potential, human breast adenocarcinoma (MCF7) and human hepatocellular carcinoma (HepG2) epithelial cell lines were used. Both of them are commonly used in toxicology and in tumoral studies. Both were recognized as good experimental models, the first one, MCF7 cell line, because of its exquisite hormone sensitivity through expression of the estrogen receptor, making it an ideal model to study hormone response and a great breast cancer representative.⁶⁶ The second one, HepG2 cells, retained inducibility and activities of several phase I and II xenobiotic metabolizing enzymes.⁶⁷ Both cell lines were obtained from the American Type Culture Collection (ATCC, Manassas, VA). MCF7 cells were cultured in a monolayer in Dulbecco's minimum essential medium, supplemented with 10% of fetal bovine serum, 100 U/mL penicillin, and 100 μ g/mL streptomycin (1%) and 2 mM L-glutamine (1%). The passages used for MCF7 are between 7 and 12. For the HepG2 cells, a minimum essential medium was used as the main culture medium with similar nutrients and proportions as those mentioned above for MCF7. The passages we used were from 9 to 14. Cells were routinely grown at 37 °C and 5% CO₂ in a humidified atmosphere.

4.5. Cytotoxicity Assays. For cytotoxicity assays, all of the compounds analyzed were dissolved in DMSO. In any case, the DMSO concentration did not exceed 0.1%, and appropriate controls of solvent were tested in all of the experiments performed. Under the same conditions, but in water, cisplatin was tested and compared to all of the compounds studied.

The exposure concentrations for the silver complexes (2–6, 9, and 10) were set from 0 to 8 μ M, prior to the wide range assayed (0–200 μ M), to determine the specific spectrum to test and the compound precipitation (data not shown). Different ranges of concentrations were tested based on their self-precipitation for phosphazene ligands **phos-1** and **phos-2** and the silver precursors. Thus, **phos1** was tested from 0 to 25 μ M, and [Ag(OTf)L] (L = PPh₃, PPh₂Me, TPA) and **phos3** were assayed from 0 to 80 μ M. The MCF7 and HepG2 cells were seeded at densities of 8×10^4 and 1×10^5 cells/mL in 96-well microplates and allowed to attach for 24 h prior to the addition of compounds under study. In each assay, all of the compounds were tested in sextuplicate/microplate, with three independent experiments being conducted to check the reproducibility and repetitivity of the results. The time of exposure of the silver complexes to the cell lines selected was 48 h at 37 °C and 5% CO₂. At the same conditions, cisplatin (0–80 μ M) was also tested.

To evaluate the cell viability, two different biomarkers were carried out, AB and NRU assays. In the AB assay, the system incorporates an oxidation–reduction (REDOX) indicator, assessing the mitochondrial ability to reduce resazurin into the fluorescent product resorufin.⁶⁸ Briefly, after 48 h of compound exposure, the AB medium was prepared by mixing a cell culture medium with a AB stock solution [resazurin sodium salt (5 mg/mL) in phosphate-buffered saline] in a 10:1 ratio (10% of the final volume). Once prepared, 100 μ L of the AB medium was added to each well containing the cells exposed to the studied compounds. The microplates were incubated at 37 °C for 2–3 h, and fluorescence was measured with a multimodal Varian Lux spectrophotometer (Thermo Scientific) with an excitation wavelength of 560 nm and an emission wavelength of 585 nm. With regard to NRU, it is a suitable end point to determine viable cells. It is based on the ability of viable cells to incorporate and bind the supravital dye neutral red in the lysosomes. This assay was performed according to Repetto et al.⁶⁹ Briefly, after a 48 h of exposure, the medium with the complexes was removed and neutral red (NR) in a fresh medium (1:100) was incorporated into each well (100 μ L) to be absorbed and concentrated in the cell lysosomes. After 3 h, the NR medium was removed, a formol-Ca₂ solution was added for 2 min, and, afterward, an acetic acid–ethanol–water mixture was also added for 15 min with continuous shaking, prior to quantitative measurement at 540 nm with a Varian Lux spectrometer (Thermo Scientific).

For both biomarkers, the cell viability was calculated using the ratio of the fluorescence/absorbance (depending on the biomarker) of treated cells to the fluorescence/absorbance of nontreated cells (control cells). All of the results are expressed as mean \pm standard deviation of the three independent experiments.

4.6. Antimicrobial Activity Assays. Determination of the MICs for Gram-Positive and Gram-Negative Strains. The antibacterial activities of all compounds were tested against the Gram-negative strains *E. coli* ATCC 10536 and *P. aeruginosa* ATCC 15442 and the Gram-positive strain *S. aureus* ATCC 11632. Bacteria were stored as glycerol stocks at –80 °C and streaked onto Luria–Bertani (LB) plates prior to each experiment. Colonies from these newly prepared plates were inoculated into 5 mL of LB media, and the tubes were incubated at 37 °C. The overnight cultures were diluted to obtain a final concentration in the experiment of approximately 5×10^5 cfu/mL. Stock solutions of each compound in DMSO were prepared at a concentration of 1 mM.

For quantitative determination of the susceptibility to all compounds, the MICs were calculated by using 2-fold serial dilutions of the compounds in a 96-well microplate. The MICs were performed according to the Clinical Laboratory Standards Institute (CLSI) methods, for Antimicrobial Susceptibility Testing.⁷⁰ The range of final concentrations tested spanned from 0.12 to 250 μ M. Bacterial growth inhibition was assessed using 0.01% resazurin added at the fifth hour of incubation at 37 °C. When a color change from blue to pink was seen in the antibiotic-free control wells, the MIC values were determined. The MIC is the lowest concentration of antimicrobial agent that prevents a color change. Each experiment was performed twice.

Determination of the MICs for *M. tuberculosis* Complex (MTBC) Strains. The compounds were assayed against two MTBC strains, *M. tuberculosis* strain H37Rv ATCC 27294 and *M. bovis* BCG Pasteur. In this work, we also utilized *M. bovis* BCG, which is commonly used as a model organism for the study of *M. tuberculosis* because it is not a virulent vaccine strain and the BCG genome shares a very high degree of similarity with that of *M. tuberculosis*. The anti-MTBC activity of all compounds was determined by the REMA (Resazurine Microtiter Assay) method according to Palomino et al.⁷¹ Stock solutions of the tested compounds were prepared in DMSO and diluted in Middlebrook 7H9 (Difco), supplemented with oleic acid, albumin, dextrose, and catalase (OADC enrichment-BBL/Becton–Dickinson), to obtain the final drug concentration range of 0.12–250 μ M of the *M. tuberculosis* strain H37Rv ATCC 27294, cultured in Middlebrook 7H9 broth, supplemented with OADC and 0.05% Tween 80. The concentration was adjusted by 5×10^5 UFC/mL, and 100 μ L of the inoculum was added to each well of the 96-well microtiter plate, together with 100 μ L of the compounds. Samples were set up in duplicate. The plate was incubated at 37 °C under a normal atmosphere. After 7 days of incubation, 30 μ L of 0.01% resazurin (solubilized in water) was added to each well, and the plate was reincubated for 24 h. A change in color from blue to pink indicated the growth of bacteria, and the MIC was defined as the lowest concentration of drug that prevented this change in color. For the resazurin solution, a resazurin sodium salt (Sigma-Aldrich) stock solution of 0.01 g was dissolved in 100 mL of sterile distilled water and sterilized by filtration.

■ ASSOCIATED CONTENT

Supporting Information

The Supporting Information is available free of charge at <https://pubs.acs.org/doi/10.1021/acs.inorgchem.9b03334>.

Tables containing details of data collection and structure refinement (Tables S1 and S2) and selected bond lengths and angles (Tables S3 and S4) for compounds 7 and 9, ³¹P and ¹H NMR spectra of compound 2 in DMSO measured over 48 h, which is the time for the biological assays (Figures S1 and S2), and a table containing the expected IC₅₀ after 24 h for metal-

lophosphazenes and their precursor exposure on MCF7 and HepG2 cells under microscope analysis (Table S5) (PDF)

Accession Codes

CCDC 1946587 and 1946588 contain the supplementary crystallographic data for this paper. These data can be obtained free of charge via www.ccdc.cam.ac.uk/data_request/cif, or by emailing data_request@ccdc.cam.ac.uk, or by contacting The Cambridge Crystallographic Data Centre, 12 Union Road, Cambridge CB2 1EZ, UK; fax: +44 1223 336033.

AUTHOR INFORMATION

Corresponding Author

Josefina Jiménez – Departamento de Química Inorgánica, Facultad de Ciencias, Instituto de Síntesis Química y Catálisis Homogénea, Universidad de Zaragoza-CSIC, 50009 Zaragoza, Spain; orcid.org/0000-0002-3444-0851; Email: jjimvil@unizar.es

Authors

Elena Gascón – Departamento de Química Inorgánica, Facultad de Ciencias, Instituto de Síntesis Química y Catálisis Homogénea, Universidad de Zaragoza-CSIC, 50009 Zaragoza, Spain

Sara Maisanaba – Departamento de Biología Molecular e Ingeniería Bioquímica, Área de Toxicología, Universidad Pablo de Olavide, 41013 Sevilla, Spain

Isabel Otal – Grupo de Genética de Micobacterias, Departamento de Microbiología, Medicina Preventiva y Salud Pública, Universidad de Zaragoza, Zaragoza 50009, Spain; Instituto de Salud Carlos III, CIBER de Enfermedades Respiratorias, E-28029 Madrid, Spain

Eva Valero – Departamento de Biología Molecular e Ingeniería Bioquímica, Área Nutrición y Bromatología, Universidad Pablo de Olavide, 41013 Sevilla, Spain

Guillermo Repetto – Departamento de Biología Molecular e Ingeniería Bioquímica, Área de Toxicología, Universidad Pablo de Olavide, 41013 Sevilla, Spain

Peter G. Jones – Institut für Anorganische und Analytische Chemie, Technische Universität Braunschweig, D-38106 Braunschweig, Germany

Complete contact information is available at:

<https://pubs.acs.org/10.1021/acs.inorgchem.9b03334>

Notes

The authors declare no competing financial interest.

ACKNOWLEDGMENTS

This work was supported by Ministerio de Economía y Competitividad (MINECO)-FEDER, under Project MAT2017-84838-P, and Gobierno de Aragón-FEDER (Groups E47_17R and B25_17R, FEDER 2014-2020 “Construyendo Europa desde Aragón”), Proyecto Puente (Grant CTM2016-76304-C2-1-R), Consejería de Economía y Conocimiento de la Junta de Andalucía 2017 (Grant CTS996 PAIDI 2018), and Project 2019-PPI1901 (VPPI-UPO). We thank Lucía Vallejo Valero for her contribution to the image design of the Table of Contents graphic.

REFERENCES

- (1) Lansdown, A. B. A pharmacological and toxicological profile of silver as an antimicrobial agent in medical devices. *Adv. Pharmacol. Sci.* **2010**, *2010*, 1–16.
- (2) For selected reviews about silver(I) complexes, see: (a) Klasen, H. J. Historical review of the use of silver in the treatment of burns. I. Early uses. *Burns* **2000**, *26*, 117–130. (b) Atiyeh, B. S.; Costagliola, M.; Hayek, S. N.; Dibo, S. A. *Effect of Silver on Burn Wound Infection Control and Healing: Review of the Literature, Burns* **2007**, *33*, 139–148. (c) Azócar, M. I.; Gómez, G.; Levín, P.; Paez, M.; Muñoz, H.; Dinamarca, N. Review: Antibacterial behavior of carboxylate silver (I) complexes. *J. Coord. Chem.* **2014**, *67*, 3840–3853. (d) Medici, S.; Peana, M.; Crisponi, G.; Nurchi, V. M.; Lachowicz, J. I.; Remelli, M.; Zoroddu, M. A. Silver coordination compounds: a new horizon in medicine. *Coord. Chem. Rev.* **2016**, *327–328*, 349–359. (e) Sim, W.; Barnard, R. T.; Blaskovich, M. A. T.; Ziora, Z. M. Antimicrobial Silver in Medicinal and Consumer Applications: A Patent Review of the Past Decade (2007–2017). *Antibiotics* **2018**, *7*, 93. (f) Liang, X.; Luan, S.; Yin, Z.; He, M.; He, C.; Yin, L.; Zou, Y.; Yuan, Z.; Li, L.; Song, X.; Lv, C.; Zhang, W. Recent advances in the medical use of silver complex. *Eur. J. Med. Chem.* **2018**, *157*, 62–80 and references cited therein.
- (3) For selected reviews about silver nanoparticles, see: (a) Rai, M.; Yadav, A.; Gade, A. Silver nanoparticles as a new generation of antimicrobials. *Biotechnol. Adv.* **2009**, *27*, 76–83. (b) Franci, G.; Falanga, A.; Galdiero, S.; Palomba, L.; Rai, M.; Morelli, G.; Galdiero, M. Silver Nanoparticles as Potential Antibacterial Agents. *Molecules* **2015**, *20*, 8856–8874. (c) Roy, A.; Bulut, O.; Some, S.; Mandal, A. K.; Yilmaz, M. D. Green synthesis of silver nanoparticles: biomolecule-nanoparticle organizations targeting antimicrobial activity. *RSC Adv.* **2019**, *9*, 2673–2702. (d) Liao, C.; Li, Y.; Tjong, S. C. Bactericidal and Cytotoxic Properties of Silver Nanoparticles. *Int. J. Mol. Sci.* **2019**, *20*, 449. (e) Some, S.; Kumar Sen, I. K.; Mandal, A.; Aslan, T.; Ustun, Y.; Yilmaz, E. Ş.; Kati, A.; Demirbas, A.; Mandal, A. K.; Ocoy, I. Biosynthesis of silver nanoparticles and their versatile antimicrobial properties. *Mater. Res. Express* **2019**, *6*, 012001.
- (4) (a) A monographic issue dedicated to bacterial resistance was published in *Chem. Rev.* **2005**, *105*, 391–774. (b) *Nat. Rev. Microbiol.* **2010**, *8*, 836.
- (5) Sierra, M. A.; Casarrubios, L.; de la Torre, M. C. Bio-Organometallic Derivatives of Antibacterial Drugs. *Chem. - Eur. J.* **2019**, *25*, 7232–7242 and references cited therein.
- (6) (a) Napoli, M.; Saturnino, C.; Cianciulli, E. I.; Varcamonti, M.; Zanfardino, A.; Tommonaro, G.; Longo, P. Silver(I) N-heterocyclic carbene complexes: Synthesis, characterization and antibacterial activity. *J. Organomet. Chem.* **2013**, *725*, 46–53. (b) Kyros, L.; Banti, C. N.; Kourkoumelis, N.; Kubicki, M.; Sainis, I.; Hadjikakou, S. K. Synthesis, characterization, and binding properties towards CT-DNA and lipoxygenase of mixed-ligand silver(I) complexes with 2-mercaptothiazole and its derivatives and triphenylphosphine. *JBIC, J. Biol. Inorg. Chem.* **2014**, *19*, 449–464.
- (7) (a) Li, X. Z.; Nikaido, H.; Williams, K. E. J. B. Silver-resistant Mutants of *Escherichia coli* Display Active Efflux of Ag⁺ and Are Deficient. *Porins* **1997**, *179*, 6127–6132. (b) Gupta, A.; Matsui, K.; Lo, J. F.; Silver, S. Molecular basis for resistance to silvercations in *Salmonella*. *Nat. Med.* **1999**, *5*, 183–188. (c) Silver, S. Bacterial silver resistance: molecular biology and uses and misuses of silver compounds. *FEMS Microbiol. Rev.* **2003**, *27*, 341–353.
- (8) Drake, P. L.; Hazelwood, K. J. Exposure-related health effects of silver and silver compounds: a review. *Ann. Occup. Hyg.* **2005**, *49*, 575–585.
- (9) (a) Aulakh, J. K.; Lobana, T. S.; Sood, H.; Arora, D. S.; Smolinski, V. A.; Duff, C. E.; Jasinski, J. P. Synthesis, structures, and ESI-mass studies of silver(I) derivatives of imidazolidine-2-thiones: Antimicrobial potential and biosafety evaluation. *J. Inorg. Biochem.* **2018**, *178*, 18–31. (b) Aulakh, J. K.; Lobana, T. S.; Sood, H.; Arora, D. S.; Kaur, R.; Singh, J.; Garcia-Santos, I.; Kaur, M.; Jasinski, J. P. Silver derivatives of multi-donor heterocyclic thioamides as antimicrobial/anticancer agents: unusual bio-activity against methicillin resistant *S. aureus*, *S. epidermidis* and *E. faecalis* and human bone cancer

MG63 cell line. *RSC Adv.* **2019**, *9*, 15470–15487. (c) Aulakh, J. K.; Lobana, T. S.; Sood, H.; Arora, D. S.; Garcia-Santos, I.; Kaur, M.; Jasinski, J. P. Synthesis, structures, and novel antimicrobial activity of silver(I) halide complexes of imidazolidine-2-thiones. *Polyhedron* **2020**, *175*, 114235. (d) Banti, C. N.; Hadjikakou, S. K. Anti-proliferative and anti-tumor activity of silver (I) compounds. *Metallomics* **2013**, *5*, 569–596 and references cited therein.

(10) For selected reviews concerning metallodrugs, see: (a) Pallavicini, P.; Dacarro, G.; Diaz-Fernandez, Y. A.; Taglietti, A. Coordination chemistry of surface-grafted ligands for antibacterial materials. *Coord. Chem. Rev.* **2014**, *275*, 37–53. (b) Medici, S.; Peana, M.; Nurchi, V. M.; Lachowicz, J. I.; Crisponi, G.; Zoroddu, M. A. Noble metals in medicine: Latest advances. *Coord. Chem. Rev.* **2015**, *284*, 329–350. (c) Klebowski, B.; Depciuch, J.; Parlinska-Wojtan, M.; Baran, J. Applications of Noble Metal-Based Nanoparticles in Medicine. *Int. J. Mol. Sci.* **2018**, *19*, 4031. (d) del Solar, V.; Contel, M. Metal-based antibody drug conjugates. Potential and challenges in their application as targeted therapies in cancer. *J. Inorg. Biochem.* **2019**, *199*, 110780.

(11) (a) Liu, W. K.; Gust, R. Metal N-heterocyclic carbene complexes as potential antitumor metallodrugs. *Chem. Soc. Rev.* **2013**, *42*, 755–773. (b) Asekunowo, P. O.; Haque, R. A.; Razali, M. R. A comparative insight into the bioactivity of mono- and binuclear silver(I)-N-heterocyclic carbene complexes: synthesis, lipophilicity and substituent effect. *Rev. Inorg. Chem.* **2017**, *37*, 29–50. (c) Johnson, N. A.; Southerland, M. R.; Youngs, W. J. Recent Developments in the Medicinal Applications of Silver-NHC Complexes and Imidazolium Salts. *Molecules* **2017**, *22*, 1263. (d) Mora, M.; Gimeno, M. C.; Visbal, R. Recent advances in gold-NHC complexes with biological properties. *Chem. Soc. Rev.* **2019**, *48*, 447–462.

(12) For a selected reviews, see: (a) Mark, J. E.; Allcock, H. R.; West, R. *Inorganic Polymers*; Prentice Hall: Englewood Cliffs, NJ, 1992; pp 61–141. (b) Allcock, H. R. *Chemistry and Applications of Polyphosphazenes*; Wiley-Interscience: Hoboken, NJ, 2003. (c) Gleria, M.; De Jaeger, R., Eds. *Synthesis and Characterization of Polyphosphazenes (Vol. I), Applicative Aspects of Polyphosphazenes (Vol. II), and Applicative Aspects of Cyclophosphazenes (Vol. III)*; Nova Science Publishers, Inc.: New York, 2004. (d) Allcock, H. R. The expanding field of polyphosphazene high polymers. *Dalton Trans.* **2016**, *45*, 1856–1862. (e) Rothmund, S.; Teasdale, I. Preparation of polyphosphazenes: a tutorial review. *Chem. Soc. Rev.* **2016**, *45*, 5200–5215. (f) Yeşilot, S.; Uslu, A. Stereochemical Aspects of Polyphosphazenes. *Polym. Rev.* **2017**, *57*, 213–247. (g) Carriedo, G. A.; de la Campa, R.; Soto, A. P. Polyphosphazenes - Synthetically Versatile Block Copolymers (“Multi-Tool”) for Self-Assembly. *Eur. J. Inorg. Chem.* **2018**, *2018*, 2484–2499.

(13) For selected and recent reviews, see: (a) Andrianov, A. K., Ed. *Polyphosphazenes for Biomedical Applications*; John Wiley & Sons, Inc.: Hoboken, NJ, 2009. (b) Ullah, R. S.; Wang, L.; Yu, H.; Abbasi, N. M.; Akram, M.; ul-Adbin, Z.; Saleem, M.; Haroon, M.; Khan, R. U. Synthesis of polyphosphazenes with different side groups and various tactics for drug delivery. *RSC Adv.* **2017**, *7*, 23363–23391. (c) Wang, L.; Yang, Y.-X.; Shi, X.; Mignani, S.; Caminade, A.-M.; Majoral, J.-P. Cyclotriphosphazene core-based dendrimers for biomedical applications: an update on recent advances. *J. Mater. Chem. B* **2018**, *6*, 884–895. (d) Magiri, R.; Mutwiri, G.; Wilson, H. L. Recent advances in experimental polyphosphazene adjuvants and their mechanisms of action. *Cell Tissue Res.* **2018**, *374*, 465–471. (e) Teasdale, I. Stimuli-Responsive Phosphorus-Based Polymers. *Eur. J. Inorg. Chem.* **2019**, *2019*, 1445–1456.

(14) See also: (a) Laurencin, C. T.; Norman, M. E.; Elgendy, H. M.; El-Amin, S. F.; Allcock, H. R.; Pucher, S. R.; Ambrosio, A. A. Use of polyphosphazenes for skeletal tissue regeneration. *J. Biomed. Mater. Res.* **1993**, *27*, 963–973. (b) Laurencin, C. T.; El-Amin, S. F.; Ibim, S. E.; Willoughby, D. A.; Attawia, M.; Allcock, H. R.; Ambrosio, A. A. A highly porous 3-dimensional polyphosphazene polymer matrix for skeletal tissue regeneration. *J. Biomed. Mater. Res.* **1996**, *30*, 133–138. (c) Langone, F.; Lora, S.; Veronese, F. M.; Caliceti, P.; Parnigotto, P. P.; Valenti, F.; Palma, G. Peripheral nerve repair using a poly-(organo)phosphazene tubular prosthesis. *Biomaterials* **1995**, *16*, 347–

353. (d) Veronese, F. M.; Marsilio, F.; Lora, S.; Caliceti, P.; Passi, P.; Orsolini, P. Polyphosphazene membranes and microspheres in periodontal diseases and implant surgery. *Biomaterials* **1999**, *20*, 91–98. (e) Henke, H.; Brüggemann, O.; Teasdale, I. Branched Macromolecular Architectures for Degradable, Multifunctional Phosphorus- Based Polymers. *Macromol. Rapid Commun.* **2017**, *38*, 1600644.

(15) (a) Andrianov, A. K.; Payne, L. G. Polymeric carriers for oral uptake of microparticulates. *Adv. Drug Delivery Rev.* **1998**, *34*, 155–170. (b) Andrianov, A. K.; Payne, L. G. Protein release from polyphosphazene matrices. *Adv. Drug Delivery Rev.* **1998**, *31*, 185–196. (c) Lakshmi, S.; Katti, D. S.; Laurencin, C. T. Biodegradable polyphosphazenes for drug delivery applications. *Adv. Drug Delivery Rev.* **2003**, *55*, 467–482. (d) Akram, M.; Wang, L.; Yu, H.; Amer, W. A.; Khalid, H.; Abbasi, N. M.; Chen, Y.; Saleem, M.; ul-Adbin, Z.; Tong, R. Polyphosphazenes as anti-cancer drug carriers: From synthesis to application. *Prog. Polym. Sci.* **2014**, *39*, 1987–2009.

(16) (a) Duncan, R. Polymer conjugates for tumour targeting and intracytoplasmic delivery. The EPR effect as a common gateway? *Pharm. Sci. Technol. Today* **1999**, *2*, 441–449. (b) Maeda, H.; Wu, J.; Sawa, T.; Matsumura, Y.; Hori, K. Tumor vascular permeability and the EPR effect in macromolecular therapeutics: a review. *J. Controlled Release* **2000**, *65*, 271–284. (c) Minko, T.; Kopeckova, P.; Kopecek, J. Efficacy of the chemotherapeutic action of HPMA copolymer-bound doxorubicin in a solid tumor model of ovarian carcinoma. *Int. J. Cancer* **2000**, *86*, 108–117. (d) Maeda, H. The enhanced permeability and retention (EPR) effect in tumor vasculature: the key role of tumor-selective macromolecular drug targeting. *Adv. Enzyme Regul.* **2001**, *41*, 189–207. (e) Maeda, H.; Sawa, T.; Konno, T. Mechanism of tumor-targeted delivery of macromolecular drugs, including the EPR effect in solid tumor and clinical overview of the prototype polymeric drug SMANCS. *J. Controlled Release* **2001**, *74*, 47–61. (f) Kopecek, J.; Kopeckova, P.; Minko, T.; Lu, Z.-R.; Peterson, C. M. Water soluble polymers in tumor targeted delivery. *J. Controlled Release* **2001**, *74*, 147–158. (g) Maeda, H.; Fang, J.; Inutsuka, T.; Kitamoto, Y. Vascular permeability enhancement in solid tumor: various factors, mechanisms involved and its implications. *Int. Immunopharmacol.* **2003**, *3*, 319–328.

(17) Delgado, C.; Francis, G. E.; Fisher, D. The uses and properties of PEG-linked proteins. *Crit. Rev. Ther. Drug Carrier Sys.* **1992**, *9*, 249–304.

(18) (a) Jiménez, J.; Laguna, A.; Gascón, E.; Sanz, J. A.; Serrano, J. L.; Barberá, J.; Oriol, L. New Liquid Crystalline Materials Based on Two Generations of Dendronised Cyclophosphazenes. *Chem. - Eur. J.* **2012**, *18*, 16801–16814. (b) Jiménez, J.; Pintre, I.; Gascón, E.; Sánchez-Somolinos, C.; Alcalá, R.; Caverio, E.; Serrano, J. L.; Oriol, L. Photoresponsive Liquid-Crystalline Dendrimers Based on a Cyclotriphosphazene Core. *Macromol. Chem. Phys.* **2014**, *215*, 1551–1562. (c) Caminade, A.-M.; Ouali, A.; Hameau, A.; Laurent, R.; Rebout, C.; Delavaux-Nicot, B.; Turrin, C.-O.; Moineau Chane-Ching, K.; Majoral, J.-P. Cyclotriphosphazene, an old compound applied to the synthesis of smart dendrimers with tailored properties. *Pure Appl. Chem.* **2016**, *88*, 919–929. (d) Caminade, A.-M.; Hameau, A.; Majoral, J.-P. The specific functionalization of cyclotriphosphazenes for the synthesis of smart dendrimers. *Dalton Trans.* **2016**, *45*, 1810–1822.

(19) (a) Allcock, H. R.; Morozowich, N. L. Bioerodible polyphosphazenes and their medical potential. *Polym. Chem.* **2012**, *3*, 578–590. (b) Mignani, S.; El Kazzouli, S.; Bousmina, M. M.; Majoral, J. P. Dendrimer Space Exploration: An Assessment of Dendrimers/Dendritic Scaffolding as Inhibitors of Protein-Protein Interactions, a Potential New Area of Pharmaceutical Development. *Chem. Rev.* **2014**, *114*, 1327–1342. (c) Mukundam, V.; Dhanunjayarao, K.; Mamidala, R.; Venkatasubbaiah, K. Synthesis, characterization and aggregation induced enhanced emission properties of tetraarylpyrazole decorated cyclophosphazenes. *J. Mater. Chem. C* **2016**, *4*, 3523–3530.

(20) (a) Allcock, H. R.; Desorcie, J. L.; Riding, G. H. The organometallic chemistry of phosphazenes. *Polyhedron* **1987**, *6*, 119–

157. (b) Chandrasekhar, V.; Thomas, K. R. J. Coordination and organometallic chemistry of cyclophosphazenes and polyphosphazenes. *Appl. Organomet. Chem.* **1993**, *7*, 1–31. (c) Chandrasekhar, V.; Nagendran, S. Phosphazenes as scaffolds for the construction of multi-site coordination ligands. *Chem. Soc. Rev.* **2001**, *30*, 193–203. (d) Chandrasekhar, V.; Krishnan, V. Advances in the chemistry of chlorocyclophosphazenes. *Adv. Inorg. Chem.* **2002**, *53*, 159–211. (e) Steiner, A.; Zacchini, S.; Richards, P. I. From neutral iminophosphoranes to multianionic phosphazenes. The coordination chemistry of imino-aza-P(V) ligands. *Coord. Chem. Rev.* **2002**, *227*, 193–216. (f) Pertici, P.; Vitulli, G.; Gleria, M.; Facchin, G.; Milani, R.; Bertani, R. Metal-Containing Poly(Organophosphazenes). *Macromol. Symp.* **2006**, *235*, 98–114.
- (21) (a) Lee, S. B.; Song, S. C.; Jin, J. I.; Sohn, Y. S. Synthesis and antitumor activity of polyphosphazene/methoxy-poly(ethylene glycol)/(diamine)platinum(II) conjugates. *Polym. J.* **1999**, *31*, 1247–1252. (b) Song, S.-C.; Lee, S. B.; Lee, B. H.; Ha, H.-W.; Lee, K.-T.; Sohn, Y. S. Synthesis and antitumor activity of novel thermosensitive platinum(II)-cyclotriphosphazene conjugates. *J. Controlled Release* **2003**, *90*, 303–311. (c) Kim, Y. S.; Song, R.; Chung, H. C.; Jun, M. J.; Sohn, Y. S. Coordination modes vs. antitumor activity: synthesis and antitumor activity of novel platinum(II) complexes of N-substituted amino dicarboxylic acids. *J. Inorg. Biochem.* **2004**, *98*, 98–104. (d) Jun, Y. J.; Kim, J. I.; Jun, M. J.; Sohn, Y. S. Selective tumor targeting by enhanced permeability and retention effect. Synthesis and antitumor activity of polyphosphazene-platinum(II) conjugates. *J. Inorg. Biochem.* **2005**, *99*, 1593–1601. (e) Song, R.; Joo Jun, Y.; Ik Kim, J.; Jin, C.; Sohn, Y. S. Synthesis, characterization, and tumor selectivity of a polyphosphazene-platinum(II) conjugate. *J. Controlled Release* **2005**, *105*, 142–150. (f) Jadhav, V. B.; Jun, Y. J.; Song, J. H.; Park, M. K.; Oh, J. H.; Chae, S. W.; Kim, I.-S.; Choi, S.-J.; Lee, H. J.; Sohn, Y. S. A novel micelle-encapsulated platinum(II) anticancer agent. *J. Controlled Release* **2010**, *147*, 144–150. (g) Avaji, P. G.; Joo, H. I.; Park, J. H.; Park, K. S.; Jun, Y. J.; Lee, H. J.; Sohn, Y. S. Synthesis and properties of a new micellar polyphosphazene-platinum(II) conjugate drug. *J. Inorg. Biochem.* **2014**, *140*, 45–52.
- (22) Henke, H.; Kryeziu, K.; Banfic, J.; Theiner, S.; Körner, W.; Brüggemann, O.; Berger, W.; Keppler, B. K.; Heffeter, P.; Teasdale, I. Macromolecular Pt(IV) Prodrugs from Poly(organo)phosphazenes. *Macromol. Biosci.* **2016**, *16*, 1239–1249.
- (23) (a) Wisian-Neilson, P.; García-Alonso, F. J. Coordination of poly(methylphenylphosphazene) and poly(dimethylphosphazene). *Macromolecules* **1993**, *26*, 7156–7160. (b) García-Alonso, F. J.; Wisian-Neilson, P. Backbone Coordination of Poly(alkyl/arylphosphazenes). *Polym. Prepr.* **1993**, *34* (1), 264–265. (c) Chen-Yang, Y. W.; Hwang, J. J.; Kau, J. Y. Polybisaminophosphazene-Silver Nitrate Complexes: Coordination and Properties. *J. Polym. Sci., Part A: Polym. Chem.* **1997**, *35*, 1023–1031. (d) Diefenbach, U.; Cannon, A. M.; Stromburg, B. E.; Olmeijer, D. L.; Allcock, H. R. Synthesis and metal coordination of thioether containing cyclo- and poly-(organophosphazenes). *J. Appl. Polym. Sci.* **2000**, *78*, 650–661. (e) Itaya, T.; Inoue, K. Construction of hairy-rod coordination polymers with lamellar structure by self-assembling of hexakis(4-pyridylmethoxy)cyclotriphosphazene and silver alkylsulfonates. *Polyhedron* **2002**, *21*, 1573–1578. (f) Ainscough, E. W.; Brodie, A. M.; Depree, C. V.; Jameson, G. B.; Otter, C. A. Polymer Building Blocks: Self-Assembly of Silver(I) Cyclotriphosphazene Cationic Columns. *Inorg. Chem.* **2005**, *44*, 7325–7327. (g) Gonsior, M.; Antonijevic, S.; Krossing, I. Silver Complexes of Cyclic Hexachlorotriphosphazene. *Chem. - Eur. J.* **2006**, *12*, 1997–2008. (h) Ainscough, E. W.; Brodie, A. M.; Davidson, R. J.; Otter, C. A. The first coordination polymer containing a chiral cyclotriphosphazene ligand. *Inorg. Chem. Commun.* **2008**, *11*, 171–174. (i) Chandrasekhar, V.; Suriya Narayanan, R. Metalation studies of 3- and 4-pyridyloxycyclophosphazenes: metal-lamacrocycles to coordination polymers. *Dalton Trans.* **2013**, *42*, 6619–6632. (j) Ainscough, E. W.; Brodie, A. M.; Davidson, R. J.; Jameson, G. B.; Otter, C. A. Flexible pyridyloxy-substituted cyclotriphosphazene platforms linked by silver(I). *CrystEngComm* **2013**, *13*, 4379–4385. (k) Gutowska, N.; Seliger, P.; Andrijewski, G.; Siwy, M.; Malecka, M.; Kusz, J. Single and double crown macrocyclic derivatives of cyclotriphosphazene as receptors of silver(I) ions. *RSC Adv.* **2015**, *5*, 38435–38442. (l) Davarci, D.; Gur, R.; Besli, S.; Senkuytu, E.; Zorlu, Y. Silver(I) coordination polymers assembled from flexible cyclotriphosphazene ligand: structures, topologies and investigation of the counteranion effects. *Acta Crystallogr., Sect. B: Struct. Sci., Cryst. Eng. Mater.* **2016**, *B72*, 344–356.
- (24) (a) Richards, P. I.; Steiner, A. Cyclophosphazenes as Nodal Ligands in Coordination Polymers. *Inorg. Chem.* **2004**, *43*, 2810–2817. (b) Benson, M. A.; Zacchini, S.; Boomishankar, R.; Chan, Y.; Steiner, A. Alkylation and Acylation of Cyclotriphosphazenes. *Inorg. Chem.* **2007**, *46*, 7097. (c) Richards, P. I.; Bickley, J. F.; Boomishankar, R.; Steiner, A. In situ recrystallisation of a coordination polymer with hemilabile linkers. *Chem. Commun.* **2008**, 1656–1658.
- (25) (a) Jiménez, J.; Laguna, A.; Benouazzane, M.; Sanz, J. A.; Díaz, C.; Valenzuela, M. L.; Jones, P. G. Metallocyclo- and Polyphosphazenes Containing Gold or Silver: Thermolytic Transformation into Nanostructured Materials. *Chem. - Eur. J.* **2009**, *15*, 13509. (b) Díaz, C.; Valenzuela, M. L.; Laguna, A.; Lavayen, V.; Jiménez, J.; Power, L. A.; O'Dwyer, C. Metallophosphazene Precursor Routes to the Solid-State Deposition of Metallic and Dielectric Microstructures and Nanostructures on Si and SiO₂. *Langmuir* **2010**, *26* (12), 10223–10233.
- (26) (a) Wang, M.; Fu, J.; Huang, D.; Zhang, C.; Xu, Q. Silver nanoparticles-decorated polyphosphazene nanotubes: synthesis and applications. *Nanoscale* **2013**, *5*, 7913–7919. (b) Fu, J.; Wang, M.; Zhang, C.; Xu, Q.; Huang, X.; Tang, X. Controlled fabrication of noble metal nanoparticles loaded on the surfaces of cyclotriphosphazene-containing polymer nanotubes. *J. Mater. Sci.* **2012**, *47*, 1985–1991.
- (27) Chandrasekhar, V.; Vivekanandan, K.; Nagendran, S.; Senthil Andavan, G. T.; Yarbrough, J. C.; Cordes, A. W. Cycloalkylamino-cyclo- and Polyphosphazenes: X-ray Crystal Structures of gem-Tetrakis(cyclohexylamino)dichlorocyclotriphosphazene and Octakis(cyclopropylamino)-cyclotriphosphazene. *Inorg. Chem.* **1998**, *37*, 6192–6198.
- (28) Bickley, J. F.; Bonar-Law, R.; Lawson, G. T.; Richards, P. I.; Rivals, F.; Steiner, A.; Zacchini, S. Supramolecular variations on a molecular theme: the structural diversity of phosphazenes (RNH)₆P₃N₃ in the solid state. *Dalton Trans.* **2003**, 1235–1244.
- (29) (a) Ford, C. T.; Dickson, F. E.; Bezman, I. I. Positional and cis-trans Isomeric Dimethylaminotriphosphonitriles. The Use of ¹H Nuclear Magnetic Resonance in Configurational Analysis. *Inorg. Chem.* **1964**, *3*, 177–182. (b) Keat, R.; Shaw, R. A. Phosphorus-Nitrogen Compounds. Part IX. The Reaction of Dimethylamine with Hexachlorocyclotriphosphazatriene: The Replacement Pattern and the Structure of the Products. *J. Chem. Soc.* **1965**, 2215.
- (30) (a) Allen, C. W. Regio- and stereochemical control in substitution reactions of cyclophosphazenes. *Chem. Rev.* **1991**, *91*, 119–135. (b) Shaw, R. A. The Reactions of Halogenocyclophosphazenes with Nitrogenous Bases. *Z. Naturforsch., B: J. Chem. Sci.* **1976**, *31*, 641–667. (c) Krishnamurthy, S. S.; Sau, A. C.; Woods, M. Cyclophosphazenes. *Adv. Inorg. Chem. Radiochem.* **1978**, *21*, 41–112.
- (31) (a) Brandt, K.; Porwollik-Czomperlik, I.; Siwy, M.; Kupka, T.; Shaw, R. A.; Davies, D. B.; Hursthouse, M. B.; Sykara, G. D. Thermodynamic vs Supramolecular Effects in the Regiocontrol of the Formation of New Cyclotriphosphazene-Containing Chiral Ligands with 1,1'-Binaphthyl Units: Spiro vs Ansa Substitution at the N₃P₃ Ring. *J. Am. Chem. Soc.* **1997**, *119*, 12432–12440. (b) Wu, H.; Meng, S. ³¹P NMR Analysis of Cyclotriphosphazenes. *Ind. Eng. Chem. Res.* **1998**, *37*, 675–683. (c) McIntosh, M. B.; Hartle, T. J.; Allcock, H. R. Synthesis and Reactivity of Alkoxy, Aryloxy, and Dialkylamino Phosphazene Azides. *J. Am. Chem. Soc.* **1999**, *121*, 884–885.
- (32) In the cases of **phos-1** and **phos-2**, the characterization data agree with those reported in the literature. See refs 27–29. In addition, selective decoupling NMR experiments and two-dimensional heteronuclear (HSQC ¹H–¹³C) correlations were made by us to give a complete characterization and to assign the signals

corresponding to the cyclohexylamino units, specifically those of N-H and NH-CH. See the [Experimental Section](#).

(33) (a) Ramachandran, K.; Allen, C. W. (Vinylxy)-chlorocyclotriphosphazenes. *Inorg. Chem.* **1983**, *22*, 1445–1448. (b) Chen-Yang, Y. W.; Chien, W. S.; Chung, J. R. The synthesis, characterization and reaction of (propargyloxy)-chlorocyclotriphosphazenes. *Polyhedron* **1989**, *8*, 1517–1522. (c) Uslu, A.; Güvenaltin, S. The investigation of structural and thermosensitive properties of new phosphazene derivatives bearing glycol and amino acid. *Dalton Trans.* **2010**, *39*, 10685–10691.

(34) Jiménez, J.; Callizo, L.; Serrano, J. L.; Barberá, J.; Oriol, L. Mixed-Substituent Cyclophosphazenes with Calamitic and Polycatenar Mesogens. *Inorg. Chem.* **2017**, *56*, 7907–7921.

(35) The additional splitting and broadening are attributed to longer range coupling to the more distant phosphorus atoms and to the quadrupole broadening by the adjacent nitrogen atom. See ref 29.

(36) (a) Lawrance, G. A. Coordinated Trifluoromethanesulfonate and Fluorosulfate. *Chem. Rev.* **1986**, *86*, 17–33. (b) Johnston, D. H.; Shriver, D. F. Vibrational Study of the Trifluoromethanesulfonate Anion: Unambiguous Assignment of the Asymmetric Stretching Modes. *Inorg. Chem.* **1993**, *32*, 1045–1047.

(37) (a) Bardaji, M.; Crespo, O.; Laguna, A.; Fischer, A. K. Structural characterization of silver (I) complexes $[Ag(O_3SCF_3)(L)]$ ($L = PPh_3, PPh_2Me, SC_4H_8$) and $[AgL_n](CF_3SO_3)$ ($n = 2-4$, $L = PPh_3, PPh_2Me$). *Inorg. Chim. Acta* **2000**, *304*, 7–16. (b) Jiménez, J.; Laguna, A.; Benouazzane, M.; Sanz, J. A.; Díaz, C.; Valenzuela, M. L.; Jones, P. G. Metallocyclo- and Polyphosphazenes Containing Gold or Silver: Thermolytic Transformation into Nanostructured Materials. *Chem. - Eur. J.* **2009**, *15*, 13509–13520.

(38) (a) Contel, M.; Jiménez, J.; Jones, P. G.; Laguna, A.; Laguna, M. Mesitylgold complexes: synthesis and reactivity; crystal structure of $[[(Ph_3P)Au(\mu-mes)Ag(tht)]_2][SO_3CF_3]_2$ ($mes = mesityl$, $tht = tetrahydrothiophene$). *J. Chem. Soc., Dalton Trans.* **1994**, *17*, 2515–2518. (b) Terroba, R.; Hursthouse, M. B.; Laguna, M.; Mendia, A. Unexpected diastereoisomeric-trimers in the crystalline structure of triflatetraphenylphosphinesilver(I). *Polyhedron* **1999**, *18*, 807–810.

(39) Mohr, F.; Falvello, L. R.; Laguna, M. A Silver(I) Coordination Polymer Containing Tridentate N- and P-Coordinating 1,3,5-Triaza-7-phosphaadamantane (PTA) Ligands. *Eur. J. Inorg. Chem.* **2006**, *2006*, 3152–3154.

(40) The two sets of resonances of two AB_2 spin systems corresponding to the phosphazene phosphorus atoms are marked in [Figure 4a](#) with symbols (● and ◆).

(41) The two sets of two doublets corresponding to the phosphane phosphorus atoms are marked in [Figure 4a](#) with symbols (*) and (○).

(42) (a) Cingolani, A.; Effendy; Marchetti, F.; Pettinari, C.; Skelton, B. W.; White, A. H. Synthesis and structural systematics of mixed triphenylphosphine/imidazole base adducts of silver(I) oxanion salts. *J. Chem. Soc., Dalton Trans.* **1999**, 4047–4055. (b) Bardaji, M.; Barrio, M.; Espinet, P. Photosensitive azobispyridine gold(I) and silver(I) complexes. *Dalton Trans.* **2011**, *40*, 2570–2577. (c) Johnson, A.; Marzo, I.; Gimeno, M. C. Ylide Ligands as Building Blocks for Bioactive Group 11 Metal Complexes. *Chem. - Eur. J.* **2018**, *24*, 11693–11702.

(43) Lawson, G. T.; Rivals, F.; Tascher, M.; Jacob, C.; Bickley, J. F.; Steiner, A. *Cis*-Trihydrogen cyclotriphosphazenes—acidic anions in strongly basic media. *Chem. Commun.* **2000**, 341–342.

(44) (a) Schmidpeter, A.; Blanck, K.; Ahmed, F. R. Bis[cyclotri(A^5 -phosphazane)dienethionato]- Ni^{II} , $-Pd^{II}$ and $-Pt^{II}$ Complexes and Their Structure. *Angew. Chem., Int. Ed. Engl.* **1976**, *15*, 488–489. (b) Allen, R. W.; O'Brien, J. P.; Allcock, H. R. Crystal and Molecular Structure of a Platinum-Cyclophosphazene Complex: *cis*-Dichloro-[octa-(methylamino)cyclotetraphosphazene-N, N “]platinum (II). *J. Am. Chem. Soc.* **1977**, *99*, 3987–3991. (c) Thomas, K. R. J.; Chandrasekhar, V.; Pal, P.; Scott, S. R.; Hallford, R.; Cordes, A. W. Unusual Tridentate N_3 Capping Coordination Behavior of Hexakis(3,5-dimethylpyrazolyl)cyclotriphosphazene, $N_3P_3(3,5-Me_2Pz)_6$: Synthesis, Spectroscopy, and Electrochemistry of Mono- and Dinuclear Copper(II) Complexes and the X-ray Structure of $N_3P_3(3,5-$

$Me_2Pz)_6^*CuCl_2$. *Inorg. Chem.* **1993**, *32*, 606–611. (d) Chandrasekhar, V.; Krishnan, V.; Steiner, A.; Bickley, J. Cyclotriphosphazene Hydrazides as Efficient Multisite Coordination Ligands. η^3 -fac-non-geminal- N_3 Coordination of spiro- $N_3P_3[O_2C_{12}H_8][N(Me)NH_2]_4$ (L) in L_2CoCl_3 and $L_2M(NO_3)_2$ ($M = Ni, Zn, Cd$). *Inorg. Chem.* **2004**, *43*, 166–172. (e) Richards, P. I.; Lawson, G. T.; Bickley, J. F.; Robertson, C. M.; Iggo, J. A.; Steiner, A. Polyanionic Ligand Platforms for Methyl- and Dimethylaluminum Arrays. *Inorg. Chem.* **2019**, *58*, 3355–3363.

(45) (a) Trotter, J.; Whitlow, S. H. Crystal structure of bis(octamethylcyclotetraphosphonitrium) tetrachlorocobaltate(II), $[(NPM_2)_4H]_2CoCl_4$. *J. Chem. Soc. A* **1970**, 460–464. (b) Chandrasekaran, A. A salt of a protonated (amino)spirocyclic cyclotriphosphazene. *Acta Crystallogr., Sect. C: Cryst. Struct. Commun.* **1994**, *C50*, 1692–1694. (c) Richards, P. I.; Benson, M. A.; Steiner, A. *In situ* complexation of lithium chloride by amphiprotic cyclophosphazenes. *Chem. Commun.* **2003**, 1392–1393. (d) Craven, M.; Yahya, R.; Kozhevnikova, E.; Boomishankar, R.; Robertson, C. M.; Steiner, A.; Kozhevnikov, I. Novel polyoxometalate-phosphazene aggregates and their use as catalysts for biphasic oxidations with hydrogen peroxide. *Chem. Commun.* **2013**, *49*, 349–351. (e) Benson, M. A.; Zacchini, S.; Boomishankar, R.; Chan, Y.; Steiner, A. Alkylation and Acylation of Cyclotriphosphazenes. *Inorg. Chem.* **2007**, *46*, 7097–7108. (f) Benson, M. A.; Ledger, J.; Steiner, A. Zwitterionic Phosphazanium Phosphazenate Ligands. *Chem. Commun.* **2007**, 3823–3825.

(46) (a) Craig, D. P.; Maccoll, A.; Nyholm, R. S.; Orgel, L. E.; Sutton, L. E. Chemical bonds involving *d*-orbitals. Part I. *J. Chem. Soc.* **1954**, 332–353. (b) Searle, H. T.; Dyson, J.; Ranganathan, T. N.; Paddock, N. L. Preparation and donor properties of the cyclic methylphosphazenes. *J. Chem. Soc., Dalton Trans.* **1975**, 203–208. (c) Gallicano, K. D.; Paddock, N. L.; Rettig, S. J.; Trotter, J. 1-Pyrazolylphosphazenes and their metal complexes. *Inorg. Nucl. Chem. Lett.* **1979**, *15*, 417–420.

(47) (a) Ott, I.; Koch, T.; Shorafa, H.; Bai, Z.; Poeckel, D.; Steinhilber, D.; Gust, R. Synthesis, cytotoxicity, cellular uptake and influence on eicosanoid metabolism of cobalt-alkyne modified fructoses in comparison to auranofin and the cytotoxic COX inhibitor Co-ASS. *Org. Biomol. Chem.* **2005**, *3*, 2282–2286. (b) Ortego, L.; Cardoso, F.; Martins, S.; Fillat, M. F.; Laguna, A.; Meireles, M.; Villacampa, M. D.; Gimeno, M. C. Strong inhibition of thioredoxin reductase by highly cytotoxic gold(I) complexes. DNA binding studies. *J. Inorg. Biochem.* **2014**, *130*, 32–37.

(48) Goitia, H.; Nieto, Y.; Villacampa, M. D.; Kasper, C.; Laguna, A.; Gimeno, M. C. Antitumoral Gold and Silver Complexes with Ferrocenyl-Amide Phosphines. *Organometallics* **2013**, *32*, 6069–6078.

(49) (a) Poyraz, M.; Banti, C. N.; Kourkoumelis, N.; Dokorou, V.; Manos, M. J.; Simic, M.; Golic-Grdadolnik, S.; Mavromoustakos, T.; Giannoulis, A. D.; Verginadis, I. I.; Charalabopoulos, K.; Hadjikakou, S. K. Synthesis, structural characterization and biological studies of novel mixed ligand Ag(I) complexes with triphenylphosphine and aspirin or salicylic acid. *Inorg. Chim. Acta* **2011**, *375*, 114–121. (b) Banti, C. N.; Giannoulis, A. D.; Kourkoumelis, N.; Owczarzak, A. M.; Poyraz, M.; Kubicki, M.; Charalabopoulos, K.; Hadjikakou, S. K. Mixed ligand-silver(I) complexes with anti-inflammatory agents which can bind to lipoxigenase and calf-thymus DNA, modulating their function and inducing apoptosis. *Metallomics* **2012**, *4*, 545–560.

(50) Galal, S. A.; Hegab, K. H.; Kassab, A. S.; Rodriguez, M. L.; Kerwin, S. M.; El-Khamry, A. M. A.; El Diwani, H. I. New transition metal ion complexes with benzimidazole-5-carboxylic acid hydrazides with antitumor activity. *Eur. J. Med. Chem.* **2009**, *44*, 1500–1508.

(51) Teyssot, M.-L.; Jarrousse, A.-S.; Manin, M.; Chevy, A.; Roche, S.; Norre, F.; Beaudoin, C.; Morel, L.; Boyer, D.; Mahiou, R.; Gautier, A. Metal-NHC complexes: a survey of anti-cancer properties. *Dalton Trans.* **2009**, 6894–6902.

(52) Haque, R. A.; Budagumpi, S.; Zetty Zulikha, H.; Hasanudin, N.; Khadeer Ahamed, M. B.; Abdul Majid, A. M. S. Silver(I)-N-heterocyclic carbene complexes of nitrile-functionalized imidazol-2-ylidene ligands as anticancer agents. *Inorg. Chem. Commun.* **2014**, *44*, 128–133.

- (53) (a) Hackenberg, F.; Lally, G.; Müller-Bunz, H.; Paradisi, F.; Quaglia, D.; Streciwilk, W.; Tacke, M. Novel symmetrically p-benzyl-substituted 4,5-diaryl-imidazole N-heterocyclic carbene-silver(I) acetate complexes. Synthesis and biological evaluation. *J. Organomet. Chem.* **2012**, *717*, 123–134. (b) Hackenberg, F.; Lally, G.; Müller-Bunz, H.; Paradisi, F.; Quaglia, D.; Streciwilk, W.; Tacke, M. Synthesis and biological evaluation of N-heterocyclic carbene-silver(I) acetate complexes derived from 4,5-ditolyl-imidazole. *Inorg. Chim. Acta* **2013**, *395*, 135–144. (c) Streciwilk, W.; Cassidy, J.; Hackenberg, F.; Müller-Bunz, H.; Paradisi, F.; Tacke, M. Synthesis, cytotoxic and antibacterial studies of p-benzyl-substituted NHC-silver(I) acetate compounds derived from 4,5-di-p-diisopropylphenyl- or 4,5-di-p-chlorophenyl-1H-imidazole. *J. Organomet. Chem.* **2014**, *749*, 88–99.
- (54) Yilmaz, V. T.; Gocmen, E.; Icel, C.; Cengiz, M.; Susluer, S. Y.; Buyukgungor, O. Synthesis, crystal structures, in vitro DNA binding, antibacterial and cytotoxic activities of new di- and polynuclear silver(I) saccharinate complexes with tertiary monophosphanes. *J. Photochem. Photobiol., B* **2014**, *131*, 31–42.
- (55) Yilmaz, V. T.; Gocmen, E.; Icel, C.; Cengiz, M.; Susluer, S. Y.; Buyukgungor, O. Di- and polynuclear silver(I) saccharinate complexes of tertiary diphosphane ligands: synthesis, structures, in vitro DNA binding, and antibacterial and anticancer properties. *JBIC, J. Biol. Inorg. Chem.* **2014**, *19*, 29–44.
- (56) Ortego, L.; Meireles, M.; Kasper, C.; Laguna, A.; Villacampa, M. D.; Gimeno, M. C. Group 11 complexes with amino acid derivatives: Synthesis and antitumoral studies. *J. Inorg. Biochem.* **2016**, *156*, 133–144.
- (57) (a) McCann, M.; Coyle, B.; McKay, S.; McCormack, P.; Kavanagh, K.; Devereux, M.; McKee, V.; Kinsella, P.; O'Connor, R.; Clynes, M. Synthesis and X-ray crystal structure of [Ag(phendio)₂]-ClO₄ (phendio = 1,10-phenanthroline-5,6-dione) and its effects on fungal and mammalian cells. *BioMetals* **2004**, *17*, 635–645. (b) Deegan, C.; Coyle, B.; McCann, M.; Devereux, M.; Egan, D. A. *In vitro* anti-tumour effect of 1,10-phenanthroline-5,6-dione (phendione), [Cu(phendione)₃](ClO₄)₂·4H₂O and [Ag(phendione)₂]-ClO₄ using human epithelial cell lines. *Chem.-Biol. Interact.* **2006**, *164*, 115–125.
- (58) Thati, B.; Noble, A.; Creaven, B. S.; Walsh, M.; McCann, M.; Kavanagh, K.; Devereux, M.; Egan, D. A. RETRACTED: *In vitro* anti-tumour and cyto-selective effects of coumarin-3-carboxylic acid and three of its hydroxylated derivatives, along with their silver-based complexes, using human epithelial carcinoma cell lines. *Cancer Lett.* **2007**, *248*, 321–331.
- (59) Thati, B.; Noble, A.; Creaven, B. S.; Walsh, M.; McCann, M.; Devereux, M.; Kavanagh, K.; Egan, D. A. Role of cell cycle events and apoptosis in mediating the anti-cancer activity of a silver(I) complex of 4-hydroxy-3-nitro-coumarin-bis(phenanthroline) in human malignant cancer cells. *Eur. J. Pharmacol.* **2009**, *602*, 203–214.
- (60) Yilmaz, V. T.; Icel, C.; Batur, J.; Aydinlik, S.; Sahinturk, P.; Aygun, M. Structures and biochemical evaluation of silver(I) 5,5-diethylbarbiturate complexes with bis(diphenylphosphino)alkanes as potential antimicrobial and anticancer agents. *Eur. J. Med. Chem.* **2017**, *139*, 901–916.
- (61) Silva-Tarouca, M. S. E.; Wolf, G.; Mueller, R. S. Determination of minimum inhibitory concentrations for silver sulfadiazine and other topical antimicrobial agents against strains of *Pseudomonas aeruginosa* isolated from canine otitis externa. *Vet. Dermatol.* **2019**, *30*, 145–150.
- (62) (a) Yilmaz, V. T.; Icel, C.; Batur, J.; Aydinlik, S.; Sahinturk, P.; Aygun, M. Structures and biochemical evaluation of silver(I) 5,5-diethylbarbiturate complexes with bis(diphenylphosphino)alkanes as potential antimicrobial and anticancer agents. *Eur. J. Med. Chem.* **2017**, *139*, 901–916. (b) Nomiya, K.; Takahashi, S.; Noguchi, R. Synthesis and crystal structure of a hexanuclear silver(I) cluster [Ag(Hmna)]₆·4H₂O (H₂ mna = 2-mercaptocotinic acid) and a supramolecular gold(I) complex H[Au(Hmna)₂] in the solid state, and their antimicrobial activities. *J. Chem. Soc., Dalton Trans.* **2000**, 2091–2097. (c) Jaros, S. W.; Guedes da Silva, M. F. C.; Krol, J.; Conceição Oliveira, M.; Smolenski, P.; Pombeiro, A. J. L.; Kirillov, A. M. Bioactive Silver-Organic Networks Assembled from 1,3,5-Triaza-7-phosphaadamantane and Flexible Cyclohexanecarboxylate Blocks. *Inorg. Chem.* **2016**, *55*, 1486–1496. Nomiya, K.; Kasuga, N. C.; Takayama, A. Synthesis, structure and antimicrobial activities of polymeric and nonpolymeric silver and other metal complexes. In *Polymeric Materials with Antimicrobial Activity: from Synthesis to Applications*; Munoz-Bonilla, A., Cerrada, M. L., Fernandez-Garcia, M., Eds.; RSC Publishing: Cambridge, U.K., 2014; pp 156–207.
- (63) Mohr, F.; Sanz, S.; Tiekink, E. R. T.; Laguna, M. Water-Soluble and Water-Stable Organometallic Gold(II) Complexes. *Organometallics* **2006**, *25*, 3084–3087.
- (64) Sheldrick, G. M. SHELXT-Integrated space-group and crystal-structure determination. *Acta Crystallogr., Sect. A: Found. Adv.* **2015**, *C71*, 3–8.
- (65) Spek, A. L. Structure validation in chemical crystallography. *Acta Crystallogr., Sect. D: Biol. Crystallogr.* **2009**, *D65*, 148–155.
- (66) Holliday, D. L.; Speirs, V. Choosing the right cell line for breast cancer research. *Breast Cancer Res.* **2011**, *13*, 215–222.
- (67) Knasmüller, S.; Mersch-Sundermann, V.; Kevekordes, S.; Darroudi, F.; Huber, W. W.; Hoelzl, C.; Bichler, J.; Majer, B. J. Use of human-derived liver cell lines for the detection of environmental and dietary genotoxins; current state of knowledge. *Toxicology* **2004**, *198*, 315–328.
- (68) Tahara, H.; Matsuda, S.; Yamamoto, Y.; Yoshizawa, H.; Fujita, M.; Katsuoka, Y.; Kasahara, T. High-content image analysis (HCIA) assay has the highest correlation with direct counting cell suspension compared to the ATP, WST-8 and Alamar blue assays for measurement of cytotoxicity. *J. Pharmacol. Toxicol. Methods* **2017**, *88*, 92–99.
- (69) Repetto, G.; del Peso, A.; Zurita, J. L. Neutral red uptake assay for the estimation of cell viability/cytotoxicity. *Nat. Protoc.* **2008**, *3*, 1125–1131.
- (70) CLSI. *Performance Standards for Antimicrobial Susceptibility Testing*, 29th ed.; CLSI supplement M100; Clinical and Laboratory Standards Institute: Wayne, PA, 2019.
- (71) Palomino, J. C.; Martin, A.; Camacho, M.; Guerra, H.; Swings, J.; Portaels, F. Resazurin microtiter assay plate: simple and inexpensive method for detection of drug resistance in *Mycobacterium tuberculosis*. *Antimicrob. Agents Chemother.* **2002**, *46*, 2720–2722.